FUDMA Journal of Sciences (FJS)
ISSN online: 2616-1370
ISSN print: 2645 - 2944
Vol. 10 No. 17, September, 2026, pp 315 – 343
DOI: https://doi.org/10.33003/fjs-2026-1017-6060

The Log-New Generalized Odd Fréchet-Weibull Distribution: Theory, Survival Regression, and Applications to Cervical Cancer and Radiation Data

***Ibrahim Abubakar Sadiq and Sani Ibrahim Doguwa**

Department of Statistics, Ahmadu Bello University, 810107 Zaria, Nigeria

*Corresponding authors' email: isabubakar@abu.edu.ng

Received: 17 Sept. 2026
Accepted: 19 Sept. 2026
Published: 25 Sept. 2026

ABSTRACT

Radiation-response and cancer-survival data often exhibit skewness, complex hazard structures, and heterogeneous covariate effects that may not be adequately represented by conventional lifetime distributions. This study develops the Log-New Generalized Odd Fréchet-Weibull (log-NGOF-W) distribution and its survival regression extension, the log-NGOF-Weibull survival regression (log-NGOF-WSR) model, to provide a flexible framework for modelling such data. The mathematical contribution is the formulation and investigation of a new log-transformed lifetime distribution and its regression structure, including their inferential and diagnostic properties. The proposed distribution is applied to three radiation datasets: F1 adult counts in peppermint packets, F1 adult susceptibility index, and feeding duration of *Stegobium paniceum*. The model provides competitive fits across the datasets, although the best-fitting distribution varies by dataset. For cervical cancer, survival data from 347 patients treated at Ahmadu Bello University Teaching Hospital, Zaria, were analysed using the log-NGOF-WSR, log-NGOF-Et-WSR, and log-WSR models. The log-NGOF-WSR model had the lowest AIC (348.63) and BIC (460.26), compared with 449.62 and 565.10 for log-NGOF-Et-WSR and 366.52 and 466.61 for log-WSR, respectively. At the 5% significance level, smoking history, family history, miscarriage, visitation, chemotherapy courses, treatment type, cancer stage, and age showed statistically significant associations with survival in the fitted model. These findings represent statistical associations rather than causal effects. The proposed framework provides a useful parametric alternative for lifetime and survival modelling, while its fully parametric assumptions, sensitivity to model specification and estimation, and validation on additional datasets warrant further investigation.

Keywords: Log-NGOF-Weibull Distribution, Survival Regression, Radiation Data, Cervical Cancer Survival, Kaplan-Meier Estimator, Cox-Snell Residuals, Parametric Survival Model

INTRODUCTION

Cervical cancer (CC) stands as one of the most common cancers among women globally, particularly in low- and middle-income countries (Bray *et al*., 2018). It is primarily caused by persistent infection with high-risk human papillomavirus (HPV) types (Arbyn *et al*., 2020). Early detection through screening schedules and prophylactic HPV vaccination has significantly reduced the prevalence and mortality rates in developed countries (Canfell *et al*., 2020). However, the burden of CC is still high in many parts of the world owing to limited access to healthcare services (HS) and effective screening programs (WHO, 2022).

It is clear that social determinants lead to CC burden, and the social determinants of health significantly influence CC outcomes, particularly in low- and middle-income countries (LMICs). Exposure variables such as socioeconomic status, education, and geographic location limit access to preventive measures like HPV vaccination and screening programs. For instance, rural and underserved populations often lack access to healthcare infrastructure and face cultural stigmas associated with gynaecological examinations, which contribute to late-stage diagnoses and poor outcomes (Bruni *et al*., 2016). Addressing these disparities requires targeted public health interventions, including education campaigns and mobile health units, to bridge gaps in awareness and accessibility (WHO, 2019).

Concerning the advances in HPV vaccination coverage and challenges (Kenret *et al*., 2026), HPV vaccination is a cornerstone of CC prevention, yet achieving comprehensive coverage remains a challenge in far-reaching regions. Issues such as cost, limited vaccine availability, and vaccine hesitancy hinder progress, particularly in LMICs (Egbon *et al*., 2022). Recent advancements, such as the development of single-dose HPV vaccines, have shown promise in reducing logistical and financial barriers (PATH, 2022). Additionally, global initiatives like Gavi's support for vaccination programs aim to increase coverage among underserved populations, underscoring the importance of coordinated international efforts (Lambach *et al*., 2024).

Emerging diagnostic techniques in CC screening and traditional approaches like Pap smears have been influential in reducing cervical cancer (CC) mortality, but newer technologies are demonstrating greater sensitivity and efficiency. HPV DNA testing, for instance, is more effective in detecting high-risk HPV types and pre-cancerous lesions (Arbyn *et al*., 2022). Innovations like self-sampling kits for HPV testing have further improved accessibility, especially for women in remote areas (Daponte *et al*., 2023). Integrating these diagnostic tools into national screening programs could significantly enhance early detection efforts and reduce disparities in outcomes (WHO, 2019).

There is a need for integrative approaches in survival analysis; however, advances in cervical cancer research emphasise the integration of clinical, molecular, and genetic factors into survival analysis models. Genomic profiling has identified specific mutations and pathways associated with poor

prognosis, offering opportunities to refine predictive models (Vallejo-Ruiz *et al*., 2024). Machine learning and deep learning algorithms are increasingly used to analyse complex datasets, uncover hidden patterns, and improve survival predictions (Rahimi *et al*., 2023). Such integrative approaches can enhance our sympathy for the disease and guide personalised treatment strategies (TS).

Leveraging public-private partnerships for better outcomes, public-private partnerships (PPPs) have proven effective in addressing gaps in cervical cancer (CC) prevention and treatment. Collaborative initiatives, such as the Pink Ribbon campaign, have mobilised resources to progress and advance HPV vaccination/inoculation and screening in sub-Saharan Africa (Chopra *et al*., 2019). Expanding these partnerships to include pharmaceutical companies and research institutions could accelerate the development and application of advanced survival models. Such collaborations are essential for scaling innovative programs and improving outcomes in resource-limited settings (UNICEF, 2023)

Survival analysis (SA), a branch of statistics that deals with time-to-event data, is a crucial tool in medical research for understanding patients' survival experiences and identifying prognostic factors (Collett, 2015). "Traditional models like the Kaplan-Meier estimator and the Cox proportional hazards model are widely used for survival data analysis" (Klein & Moeschberger, 2003). While the "Kaplan-Meier (K-M) estimator is non-parametric and useful for estimating survival functions, it does not account for covariates. The Cox proportional hazards model, although accounting for covariates, assumes proportional hazards, which may not always hold in clinical data" (Therneau *et al*., 2000). These limitations have led to the development of more flexible survival models to better capture the complexity of survival data (Bender *et al*., 2005).

The "New Generalized Odd Fréchet-Weibull (NGOF-Weibull) distribution" is an advanced statistical model that provides greater flexibility in modelling survival data by accommodating various hazard rate shapes (Sadiq *et al*., 2022; Sadiq *et al*., 2023a; Sadiq *et al*., 2023b; Sadiq *et al*., 2023c). This model extends the traditional Weibull distribution, allowing it to fit a wider range of survival data more accurately. It incorporates features from the Fréchet and Odd Weibull distributions, providing a robust framework for analysing time-to-event data with non-proportional hazards (Legrand, 2021). Despite advancements in survival analysis, there is a need for models that can simultaneously handle complex hazard structures and accommodate various covariates affecting survival probabilities (McGrath *et al*., 2018).

This study introduces a novel Log-New Generalised Odd Fréchet-Weibull (Log-NGOF-Weibull) distribution and its corresponding survival regression model (Log-NGOF-WSR). Recognising the complex nature of radiation and cervical cancer data, influenced by factors like exposure levels, environmental conditions, and individual responses, this research aims to develop models that can more accurately capture radiation and survival time patterns. The Log-NGOF-WSR model can identify key prognostic factors influencing cervical cancer outcomes. Additionally, the study utilises the Kaplan-Meier (K-M) estimator to benchmark the performance of the proposed models against traditional survival models, providing valuable insights into their strengths and limitations.

The Log-NGOF-Weibull distribution addresses gaps in existing survival models by offering greater flexibility in handling non-Gaussian errors, accommodating complex covariate effects, and improving predictive accuracy through a more realistic representation of survival time distributions. These advantages make it a valuable tool for researchers aiming to extract meaningful insights from diverse survival datasets.

The study objectives are as follows:

i. To develop the Log-NGOF-Weibull and Log-NGOF-WSR models that can more accurately capture radiation and cervical cancer time-to-event datasets.
ii. To fit the developed model to the dataset to assess its performance and suitability.
iii. To estimate survival probabilities using both the new model and the Kaplan-Meier estimator, comparing their effectiveness.
iv. To identify significant prognostic factors affecting cervical cancer survival using the new model.
v. To compare survival probability curves derived from the new model and the Kaplan-Meier estimator to evaluate differences and similarities.
vi. To study the residuals to assess the overall model fit and identify any deviations or patterns.

The development of the "log-NGOF-Weibull" models represents a significant advancement in survival analysis. This offers enhanced flexibility and accuracy for cervical cancer (CC) time-to-event observations/data/statistics. By addressing the limitations of traditional models and incorporating the Kaplan-Meier estimator, this study aims to provide a comprehensive tool for researchers and clinicians to better understand and predict cervical cancer outcomes. The "NGOF-Weibull model and its variants have been applied in various fields", including reliability engineering and biostatistics, to model time-to-failure data and survival times (Sadiq *et al*., 2023c). These models have demonstrated superior performance in fitting data with non-proportional hazards and providing more accurate estimates of survival probabilities compared to traditional models (Royston & Parmar, 2002).

Identifying prognostic factors is crucial for understanding the progression of cervical cancer and improving patient outcomes. Factors such as age, tumour stage, histological type, lymph node involvement, and HPV genotype have been shown to significantly influence survival in cervical cancer patients (Cooley *et al*., 2023). Advanced survival models like the NGOF-Weibull can incorporate these covariates more effectively, providing a nuanced understanding of their impact on survival (Royston & Parmar, 2002; Sadiq *et al*., 2023c).

Researchers have developed various survival regression models based on parametric distributions and applied them to diverse survival data. For instance, Table 1 presents the theoretical review of survival regression models on parametric distributions:

Table 1: Theoretical Review of Survival Regression Models on Parametric Distributions

Ref	Model/Distribution Developed	Brief Description / Application
Silva *et al*., 2009	Modified Weibull Distribution	Proposed the log-modified Weibull regression model.
Alizadeh *et al*., 2018	Log-Odd Power Cauchy-Weibull	Developed a novel survival regression model based on this distribution.
Kharazmi *et al*., 2022	Generalized Log-Logistic Class	Introduced with an associated survival regression model.
Baharith *et al*., 2020	Odds Exponential-Pareto IV	Presented with its survival regression model.
Cruz *et al*., 2016	Log-Odd Log-Logistic Weibull	Developed and applied for survival data modelling.
Alamoudi *et al*., 2017	Log-Fréchet Regression Model	Focused on estimation and application using censored data.
Hashimoto *et al*., 2012	Log-Burr XII Regression Model	Designed for grouped survival data.
Carrasco *et al*., 2008	Log-Modified Weibull Model	Applied to censored survival data.

In "recent years, scientists have proposed various flexible and robust survival regression models and distribution families to handle varying hazard shapes and a variety of real-life intricacies, for example skewness, censoring, and heavy tails" (Semary *et al*., 2025). For instance, Almarashi & Elgarhy (2023) and Jamal *et al*. (2022) introduced a modified Type II half-logistic generated-G family, emphasising its ability to improve data fitting for survival and reliability data. Similarly, Alyami *et al*. (2023) and Alyami *et al*. (2023) developed the Lifetime-G family, utilising quantile-based techniques for enhanced modelling flexibility, while Hassan *et al*. (2023) proposed the half-logistic odd power inverse moment exponential distribution and highlighted its superior fitting performance in real-life applications. These studies align with the growing emphasis on constructing families of distributions capable of modelling a variety of data characteristics, an objective that our proposed NGOF-Weibull survival regression model also seeks to achieve.

Several scholars have also developed a "broad view of the Weibull distribution" (Semary, *et al*., 2025) to address its limitations in modelling different hazard shapes. The research of Alyami *et al.* (2023) proposed the odd inverse power generalised Weibull distribution, while Yadav *et al*. (2023) explored the Topp-Leone Weibull distribution. These models offer additional shape parameters to improve model flexibility and goodness of fit. Additionally, Sadiq *et al*. (2024) introduced the Odd Rayleigh-G (OR-G) family of distributions, demonstrating superior performance across various data types due to its capability to capture a wide range of tail behaviours and hazard shapes. Similarly, Ahmad *et al*. (2023), Algarni *et al*. (2023), and Bantan *et al*. (2023) proposed the Kumaraswamy Transmuted Inverse Rayleigh Truncated Lindley distribution and the cosine-G family, respectively, both offering novel parameterisations that enhance flexibility. Our proposed NGOF-Weibull model aligns with these innovations by combining the strengths of the generalised Weibull baseline with the versatile structure of the NGOF generator to produce a model suitable for complex survival datasets.

Recent survival studies have also focused on regression modelling and practical applications. The study by Usman *et al*. (2025) applied accelerated failure time models, specifically log-logistic and Weibull survival regression models, to assess tuberculosis survival data. Their findings emphasised the suitability of Weibull-based models in capturing time-to-event dynamics in biomedical data. Their work validates the continued relevance and adaptability of the Weibull structure in survival analysis, which our research builds upon by embedding it within a more flexible NGOF-G framework. Additionally, the Odd Rayleigh-G distribution by Sadiq *et al*. (2024) demonstrated the significance of shape-enhancing generator functions in survival models, reinforcing our choice of integrating the NGOF generator into the Weibull structure to improve hazard modelling and parameter estimation efficiency.

Other scholars, such as Tahir *et al*. (2023), introduced extensions to Topp-Leone generated families, while Elbatal *et al*. (2023) proposed the alpha power transformed Weibull-G family. The paper by Cordeiro *et al*. (2023) contributed to the Sine-G distribution, highlighting the ongoing exploration of generator-based distributional frameworks. These developments demonstrate a consistent trend in statistical modelling: the integration of classical distributions with newly constructed generator mechanisms to achieve higher modelling precision. In light of these trends, the NGOF-Weibull survival regression model proposed in our study offers a significant contribution by merging a flexible generator with a robust baseline distribution, enhancing modelling capacity for censored biomedical data such as that of vesicovaginal fistula repair time.

Recent advances in survival analysis and censored regression modelling emphasise that estimator performance and model adequacy must be evaluated jointly under censoring, non-normality, and finite-sample conditions. Yenilmez *et al*. (2022) demonstrated that estimator choice plays a critical role in right-censored biomedical data, showing that weighted and parametric estimators can outperform semi-parametric alternatives depending on censoring intensity and distributional assumptions. Extending this line of work, Yenilmez and Kantar (2023) proposed exponentiated generalised censored regression models and employed Monte Carlo simulations to highlight the importance of flexible distributional forms and comprehensive finite-sample evaluation. Robustness to censoring and error misspecification has also been addressed through alternative estimation strategies, including Tobit-type regularisation (Toker *et al*., 2021) and modified maximum likelihood estimators under skewed error distributions (Açıtaş *et al*., 2021), which improve inferential reliability when classical assumptions fail. Earlier studies by Yenilmez and Kantar (2019) and Yenilmez and Kantar (2018) further emphasised the need for accommodating skewness and non-normality in censored regression through alternative likelihood-based and distribution-driven estimators. Complementary evidence from Weibull-focused research in applied contexts (Usta *et al*., 2018; Kantar *et al*., 2016; Arik *et al*., 2015; Abd Elgawad *et al*., 2025; Mohammed *et al*., 2025) demonstrated that model flexibility and estimator robustness substantially affect bias, mean squared error, and convergence behaviour, particularly in small samples and under atypical data

structures. Motivated by these findings, the present study adopts a fully parametric likelihood-based framework and employs extensive Monte Carlo simulations and information-criterion-based model comparisons to rigorously assess estimator accuracy, uncertainty quantification, and numerical stability of the proposed log-NGOF-W model relative to closely related alternatives.

Nonetheless, it is essential to look at the causal relationship between exposure factors and survival time. To capture the impact of these factors on the participants' survival, a survival regression model can be used (Semary *et al*., 2025). The innovation of creating survival regression models for continuous probability distributions can be used to address this issue (Semary *et al*., 2025). Using a regression framework, we consider a set of location-scale models in which the response N by 1 column vector Y=log(X), where $Y=(y_1, y_2, ..., y_n)^T$, is related with the $n\times p$ matrix $X=(x_1, x_2, ...x_p)^T$ of p covariates and $x_k=(x_{1k}, x_{2k}, ..., x_{nk})^T$ with $k=1, 2, ..., p$. The probability density function (PDF) of X is immediately transformed in terms of the PDF $y=\log(x); x>0$, in this section using the one-to-one Jacobian transformation, which is typically done in this situation (Semary *et al*., 2025): $g(y)=f(x)\left|\frac{dx}{dy}\right|$.

The NGOF-Weibull Distribution's PDF and Survival Function.

The NGOF-Weibull distribution was defined by the researchers (Sadiq *et al*., 2023c). If the PDF and survival function (SF) of a random variable X are provided in equations (1) and (2), respectively, then the variable is said to follow the new generalized odd Fréchet-Weibull (NGOF-Weibull) distribution for all $x;\alpha,\beta,\gamma,\phi,\omega>0$.

$$f_{ngofw}(x)=\beta\gamma\alpha^{\beta}\left(\omega\phi^{-\omega}x^{\omega-1}V\right)(1-V)^{-(\gamma+1)}\left((1-V)^{-\gamma}-1\right)^{\beta-1}\exp\left\{-\left(\alpha\left((1-V)^{-\gamma}-1\right)\right)^{\beta}\right\} \quad (1)$$

and

$$S_{ngofw}(x)=1-\exp\left\{-\left(\alpha\left((1-V)^{-\gamma}-1\right)\right)^{\beta}\right\}. \quad (2)$$

Where in the PDF and SF presented in equations (1) and (2), $V=\exp\left\{-\left(\frac{x}{\phi}\right)^{\omega}\right\}$

With α varied and all other parameters held constant, Figures 1 and 2 display the PDF and survival function graphs of this distribution, respectively.

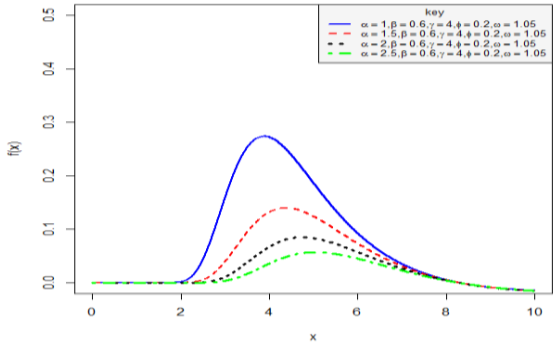

Figure 1: The Plot of the NGOF-W Distribution's PDF

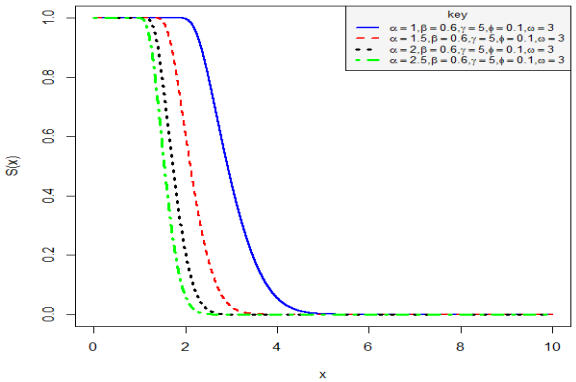

Figure 2: The plot of the NGOF-W Distribution's SF

Plotting the NGOF-Weibull distribution's PDF in Figure 1 with increasing α while holding other parameters constant allows one to examine the effects of the alpha (α) parameter. According to the influence of the distribution's form, alpha (α) mostly regulates the shape of the distribution's right tail. A heavier tail indicates a greater likelihood of finding larger values when alpha is lower $(\alpha<2)$. As alpha increases $(\alpha>2)$, the tail gets lighter, suggesting a decreased likelihood of seeing higher values, and it progressively approaches an exponential-like decline. Although alpha (α) has a minor impact on the left tail as well, the right side is where it is most noticeable.

Figure 2 shows several SF curves for the NGOF-W distribution. Each curve corresponds to a specific value of alpha (α). Since all other parameters are constant, the curves illustrate the effect of varying alpha on survival. The

curve with the highest alpha $(\alpha = 2.5)$ has a higher $S(x)$ survival probability for a given time x compared to the other curves. This means the probability of surviving beyond that time x is greater for the higher alpha. As alpha decreases $(\alpha = 2, 1.5)$, the curves shift to the right. The same $S(x)$ value is now reached at a lower x value. This indicates a lower probability of surviving beyond that time x for lower alpha (α). In essence, by keeping all other parameters constant, a higher alpha (α) in the NGOF-W distribution explains a higher probability of a system or component surviving for a longer duration.

The Construction of Logarithmic-NGOFW (Log-NGOFW) Distribution

The logarithmic transformation is introduced to place the proposed distribution within a location-scale framework on the log-time scale, which is standard in accelerated failure time (AFT) modelling. On the log scale, the baseline hazard is allowed to vary flexibly while preserving interpretability of scale effects through the parameter (ρ). In contrast to classical Weibull and Burr-type models, the log-NGOF-W formulation enables simultaneous control of tail heaviness (γ), global shape (β), and time scaling (ρ) in a unified structure.

From a statistical perspective, the log transformation stabilises numerical optimisation by reducing skewness and improving curvature of the likelihood surface, particularly under moderate to heavy right censoring. This results in improved finite-sample estimation accuracy and more reliable inference (Mohammed *et al*., 2025; Mohammed *et al*., 2025). Empirically, the advantages of the log-NGOF-W model are demonstrated through extensive Monte Carlo simulations, where it consistently outperforms closely related log-parametric competitors in terms of bias, RMSE, coverage probability, and numerical convergence.

Equation (1) defines the NGOF-Weibull density function for a random variable X. The PDF of $Y = \log(X)$, for $y \in \Re$, is obtained by substituting the scale parameter $\phi = \exp\{\mu\}$ and the shape parameter $\omega = \frac{1}{\rho}$ using the Jacobian transformation (JT):

$$g(y;\alpha,\beta,\gamma,\mu,\rho) = \frac{\beta\gamma\alpha^{\beta}}{\rho}\exp\left\{\frac{y-\mu}{\rho}\right\}\exp\left\{-\exp\left(\frac{y-\mu}{\rho}\right)\right\}\left\{1-\exp\left\{-\exp\left(\frac{y-\mu}{\rho}\right)\right\}\right\}^{-(\gamma+1)} \times\left(\left\{1-\exp\left\{-\exp\left(\frac{y-\mu}{\rho}\right)\right\}\right\}^{-\gamma}-1\right)^{\beta-1}\exp\left\{-\left(\alpha\left(\left\{1-\exp\left\{-\exp\left(\frac{y-\mu}{\rho}\right)\right\}\right\}^{-\gamma}-1\right)\right)^{\beta}\right\} \quad (3)$$

where the limit of mu is $-\infty < \mu < \infty$ and $\beta, \gamma, \alpha, \rho > 0$. The density function defined in equation (3) is termed the log-NGOF-W distribution, and the SF is derived as,

$$S(y) = 1-\exp\left\{-\left(\alpha\left(\left\{1-\exp\left\{-\exp\left(\frac{y-\mu}{\rho}\right)\right\}\right\}^{-\gamma}-1\right)\right)^{\beta}\right\} \quad (4)$$

Equation (3) allows us to recast $Z = (y-\mu)/\rho$ as a log-linear (LL) model [48]:

$$Y = \mu + \rho Z. \quad (5)$$

Figures 3 and 4, respectively, display the PDF and survival function graphs for the Log-NGOF-W model.

The plots of the PDF and survival function for the Log-NGOF-W model are presented in Figures 3 and 4, respectively.

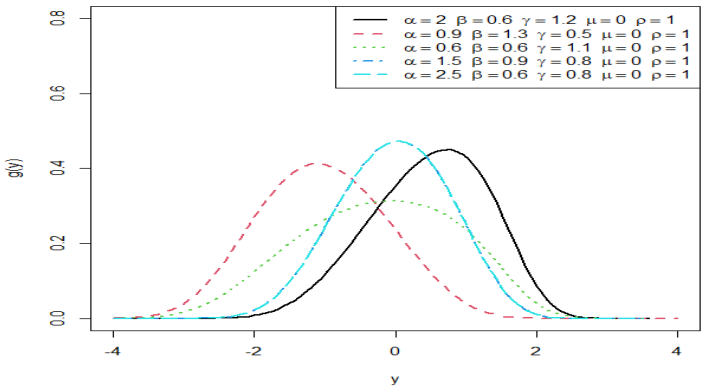

Figure 3: The Density Function plot of the Log-NGOF-W Distribution

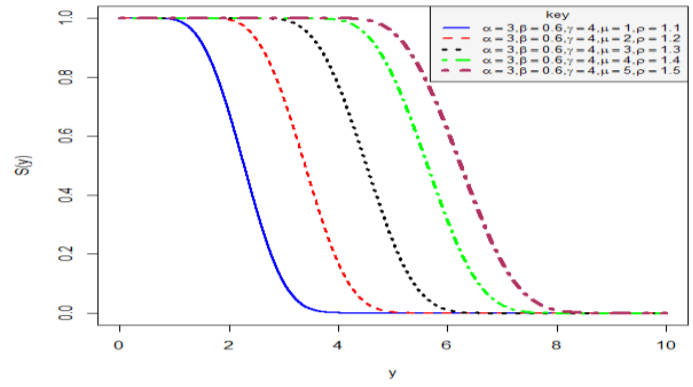

Figure 4: Survival Function (SF) plot of the Log-NGOF-W Distribution

Figure 3 illustrates a graph of the Log-NGOF-Weibull distribution as a function of y. The shape of the distribution is determined by three parameters, alpha, beta, and gamma. Alpha (α) controls the scale of the distribution. A higher alpha value results in a distribution that is stretched out to the right. Beta (β) controls the shape of the distribution. A higher beta value results in a more peaked distribution. Gamma (γ) controls the location of the distribution. A higher gamma value shifts the distribution to the right. The $y-axis$ of the plot is labelled $g(y)$, which is the PDF of the Log-NGOF-Weibull distribution. The PDF expresses how likely it is to observe a particular value of y. The area under the curve between two points represents the probability that y will fall within that range. The plot in Figure 4 shows the survival function of the Log-NGOF-Weibull distribution, which can be used to model a wide variety of survival shapes, depending on the values of the parameters. The specific shapes of the distributions in the plot are determined by the values of $\alpha, \beta, \gamma, \mu, \rho$ that are shown for each curve.

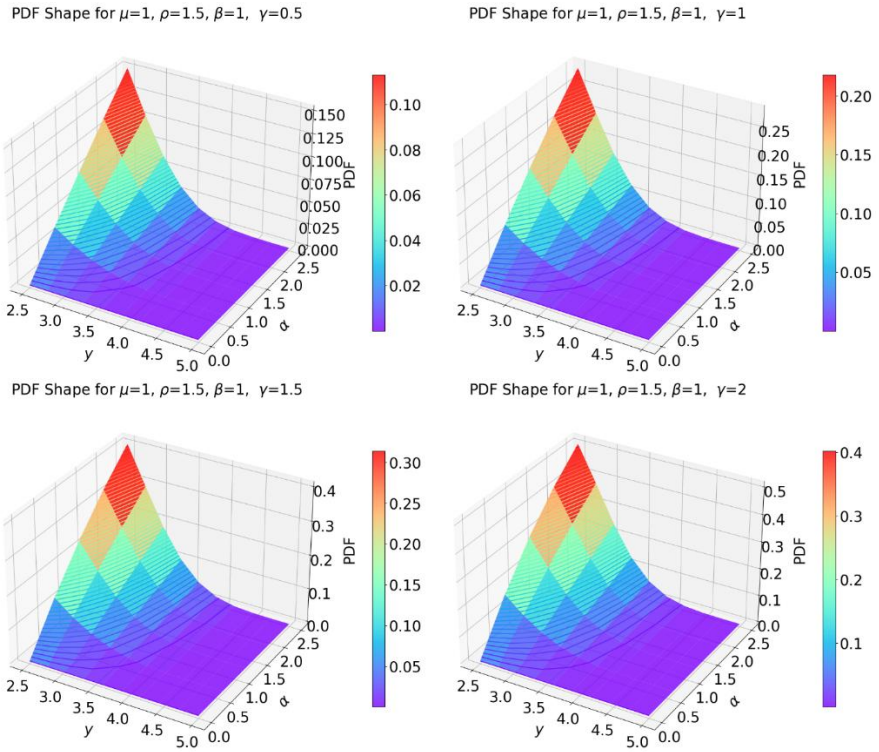

Figure 5: 3D plots of the PDF of the Log-NGOF-Weibull distribution.

Figure 5 shows the PDF shapes while maintaining the other parameters $(\mu, \rho, \text{ and } \beta)$ constant; the value of the parameter γ can vary. The following are observed:

i. Effect of γ: The parameter γ affects the shape and peak value of the PDF. As γ increases, the peak value of the PDF likewise increases. This points out that higher values of γ result in a higher probability density (PDF) at the peak.

ii. Effect of $\mu, \rho, \text{ and } \beta$: These parameters are kept constant in the plots, allowing us to isolate the influence of γ on the PDF shape. The constant values are: $\mu = 1, \rho = 1.5 \text{ and } \beta = 1$.

The figure provides a visual representation of how the PDF shape changes with varied values of γ while holding $\mu, \rho, \text{ and } \beta$ constant. Higher values of γ result in higher peak values of the PDF, indicating a higher probability density at the peak. The gradual decline in the PDF values as x and y increase is consistent across all plots. This displays the general behaviour of the distribution under varying settings.

Figure 6 shows the PDF shapes for different values of the parameter γ, while keeping the other parameters $(\mu, \rho, \text{ and } \beta)$ constant.

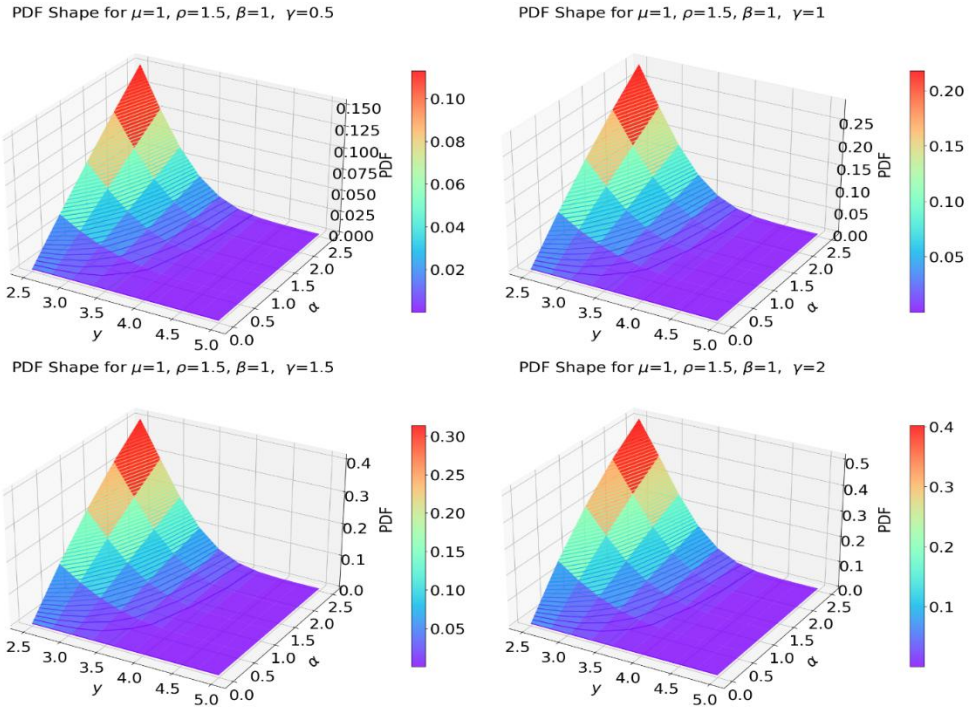

Figure 6: 3D Plots of the PDF of the Log-NGOF-W Distribution

i. Effect of γ: The parameter γ affects the shape and peak value of the PDF. As γ rises, the peak value of the PDF also increases. This points out that larger values of γ result in a larger probability density (PD) at the peak.

ii. Influence of $\mu,\ \rho,$ and β: These parameters are kept constant in the plots, allowing us to isolate the effect of γ on the PDF shape. The constant values are: $\mu = 3,\ \rho = 2$ and $\beta = 2.5$.

The figure provides a visual representation of the PDF shape changes with dissimilar values of γ while holding $\mu, \rho,$ and β constant. Higher values of γ result in higher peak values of the PDF, indicating a higher probability density at the peak. The gradual decline in the PDF values as x and y increase is consistent across all plots, showing the general behaviour of the distribution under varying conditions.

Table 2 provides a detailed view of the survival probabilities for different combinations of $\mathrm{y},\ \mu,$ and ρ. It shows that higher values of μ are associated with better survival outcomes, while higher values of ρ are associated with lower survival probabilities. The survival probabilities decrease over time (y), which is consistent with the general behaviour of survival functions.

i. The SF ($S(\mathrm{y})$): The SF, $S(\mathrm{y})$, signifies the probability that a subject will survive beyond a certain time y (Semary *et al*., 2025). Larger values of $S(\mathrm{y})$ indicate a higher probability of survival.

ii. Parameters (ρ): Table 1 shows survival functions for different values of ρ. As ρ increases, the survival probabilities generally decrease, indicating that higher values of ρ correspond to a higher hazard rate or lower survival probability.

iii. Effect of μ (mu): The parameter μ represents a location parameter. As μ increases, the survival probabilities also increase for a given y and ρ. This recommends that larger values of μ are associated with better survival outcomes.

iv. Effect of y: The variable y represents time. As y increases, the survival probabilities decrease for a given μ and ρ. This is expected, as the probability of survival typically decreases over time.

v. Comparison Across ρ values:

For $\rho = 1.5$, the survival probabilities are generally higher compared to $\rho = 2.5$ and $\rho = 3.5$.

For $\rho = 2.5$, the survival probabilities are intermediate.

For $\rho = 3.5$, the survival probabilities are the lowest, indicating the highest hazard rate among the three ρ values.

Table 2: Survival Function for the Log-NGOF-Weibull Distribution at $\alpha = 0.5$; $\beta = 1.5$, and $\gamma = 1.5$

y	μ	$\rho = 1.5$	$\rho = 2.5$	$\rho = 3.5$
		$S(y)$	$S(y)$	$S(y)$
0.5000	0.5000	0.2940	0.2940	0.2940
0.5000	1.0000	0.5537	0.4407	0.3955
0.5000	1.5000	0.8302	0.6123	0.5124
1.5000	0.5000	0.0457	0.1062	0.1462
1.5000	1.0000	0.1284	0.1830	0.2110
1.5000	1.5000	0.2940	0.2940	0.2940
2.5000	0.5000	0.0023	0.0282	0.0628
2.5000	1.0000	0.0124	0.0572	0.0977
2.5000	1.5000	0.0457	0.1062	0.1462
3.5000	0.5000	0.0000	0.0048	0.0226
3.5000	1.0000	0.0002	0.0124	0.0386
3.5000	1.5000	0.0023	0.0282	0.0628
4.5000	0.5000	0.0000	0.0004	0.0064
4.5000	1.0000	0.0000	0.0015	0.0124
4.5000	1.5000	0.0000	0.0048	0.0226
5.5000	0.5000	0.0000	0.0000	0.0013
5.5000	1.0000	0.0000	0.0001	0.0030
5.5000	1.5000	0.0000	0.0004	0.0064
6.5000	0.5000	0.0000	0.0000	0.0002
6.5000	1.0000	0.0000	0.0000	0.0005
6.5000	1.5000	0.0000	0.0000	0.0013
7.5000	0.5000	0.0000	0.0000	0.0000
7.5000	1.0000	0.0000	0.0000	0.0000
7.5000	1.5000	0.0000	0.0000	0.0002

Table 3 provides a detailed view of the survival probabilities for different combinations of $y, \mu,$ and ρ. It shows that higher values of μ are associated with better survival outcomes, while higher values of ρ are associated with lower survival probabilities. The survival probabilities decrease over time (y), which is consistent with the general behaviour of survival functions.

i. SF ($S(y)$): The SF, $S(y)$, signifies the probability that a subject will survive beyond a certain time y. Higher values of $S(y)$ indicate a higher probability of survival [48].

ii. Parameters (μ): The table shows survival functions for different values of μ. As μ increases, the survival probabilities generally increase, indicating that larger values of μ correspond to better survival outcomes.

iii. Effect of ρ (rho): The parameter ρ represents a shape parameter. As ρ increases, the survival probabilities generally decrease for a given y and μ. This suggests that larger values of ρ are associated with a higher hazard rate or lower survival probability.

iv. Effect of y: The variable y represents time. As y increases, the survival probabilities decrease for a given μ and ρ. This is expected, as the probability of survival typically decreases over time.

v. Comparison Across μ Values:

For $\mu = 2.5$, the survival probabilities are generally lower compared to $\mu = 3,\ \mu = 3.5,$ and $\mu = 4.$

For $\mu = 3$, the survival probabilities are intermediate.

For $\mu = 3.5$, the survival probabilities are higher.

For $\mu = 4$, the survival probabilities are the highest, indicating the best survival outcomes among the four μ values.

Table 3: Survival function for the Log-NGOF-Weibull distribution at $\alpha = 0.5$; $\beta = 1.5$, and $\gamma = 1.5$

y	**ρ**	**μ=2.5**	**μ=3**	**μ=3.5**	**μ=4**
0.5000	2.0000	0.7811	0.6994	0.6374	0.5902
1.5000	2.0000	0.4407	0.4140	0.3955	0.3818
2.5000	2.0000	0.1830	0.1989	0.2110	0.2203
3.5000	2.0000	0.0572	0.0788	0.0977	0.1142
4.5000	2.0000	0.0124	0.0248	0.0386	0.0526
5.5000	2.0000	0.0015	0.0057	0.0124	0.0210
6.5000	2.0000	0.0001	0.0008	0.0030	0.0070

y	ρ	μ=2.5	μ=3	μ=3.5	μ=4
7.5000	2.0000	0.0000	0.0001	0.0005	0.0018
0.5000	3.0000	0.9773	0.9255	0.8617	0.8001
1.5000	3.0000	0.7811	0.6994	0.6374	0.5902
2.5000	3.0000	0.4407	0.4140	0.3955	0.3818
3.5000	3.0000	0.1830	0.1989	0.2110	0.2203
4.5000	3.0000	0.0572	0.0788	0.0977	0.1142
5.5000	3.0000	0.0124	0.0248	0.0386	0.0526
6.5000	3.0000	0.0015	0.0057	0.0124	0.0210
7.5000	3.0000	0.0001	0.0008	0.0030	0.0070
0.5000	4.0000	0.9999	0.9959	0.9773	0.9424
1.5000	4.0000	0.9773	0.9255	0.8617	0.8001
2.5000	4.0000	0.7811	0.6994	0.6374	0.5902
3.5000	4.0000	0.4407	0.4140	0.3955	0.3818
4.5000	4.0000	0.1830	0.1989	0.2110	0.2203
5.5000	4.0000	0.0572	0.0788	0.0977	0.1142
6.5000	4.0000	0.0124	0.0248	0.0386	0.0526
7.5000	4.0000	0.0015	0.0057	0.0124	0.0210

The hazard function of the Log-NGOF-Weibull distribution, i.e., $Y \sim \text{Log-NGOF-W}(\beta,\gamma,\alpha,\rho,\mu)$ is derived as:

$$h(y;\alpha,\beta,\gamma,\mu,\rho)=\frac{\beta\gamma\alpha^{\beta}}{\rho}\exp\left\{\frac{y-\mu}{\rho}\right\}\exp\left\{-\exp\left(\frac{y-\mu}{\rho}\right)\right\}\left(1-\exp\left\{-\exp\left(\frac{y-\mu}{\rho}\right)\right\}\right)^{-(\gamma+1)}$$
$$\times\left(\left(1-\exp\left\{-\exp\left(\frac{y-\mu}{\rho}\right)\right\}\right)^{-\gamma}-1\right)\exp\left\{-\left(\alpha\left(\left(1-\exp\left\{-\exp\left(\frac{y-\mu}{\rho}\right)\right\}\right)^{-\gamma}-1\right)\right)^{\beta}\right\}$$
$$\times\left(1-\exp\left\{-\left(\alpha\left(\left(1-\exp\left\{-\exp\left(\frac{y-\mu}{\rho}\right)\right\}\right)^{-\gamma}-1\right)\right)^{\beta}\right\}\right)^{-1} \quad (6)$$

The plots and numerical analysis of the hazard function presented in equation (6) are provided in detail in Figures 7 and 8, and Tables 4 and 5, respectively.

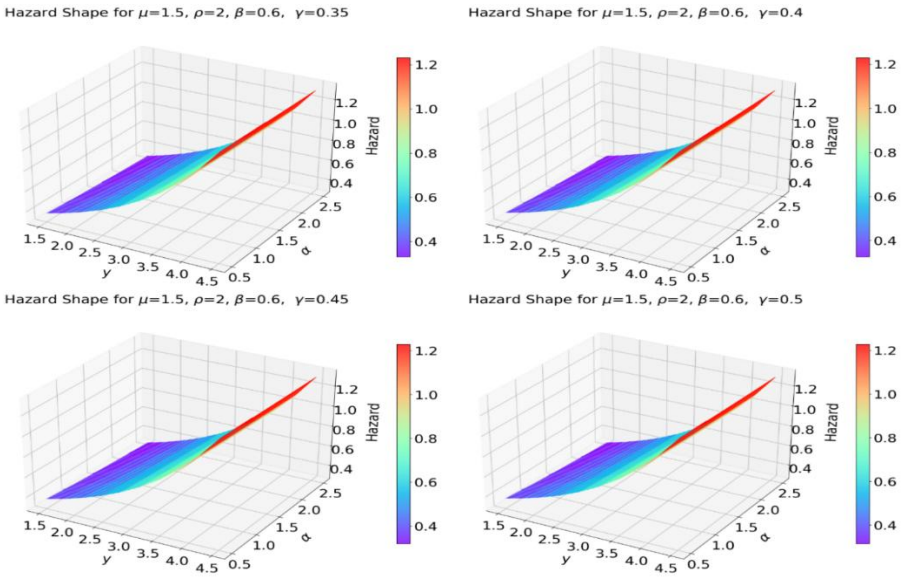

Figure 7: Four 3D plots of the HF of the Log-NGOF-Weibull Distribution

Figure 7 shows the hazard function (HF) shapes for different values of the parameter γ, while holding the other parameters $(\mu, \rho, \text{ and } \beta)$ unchanged.

i. Effect of γ (gamma): The parameter γ affects the shape and peak value of the hazard function. As γ increases, the peak value of the hazard function remains

around 1.2. This indicates that the hazard rate is relatively stable across different values of γ.

ii. Effect of μ (mu), ρ (rho), and β (beta): These parameters are kept constant in the plots, allowing us to isolate the effect of γ on the hazard function shape. The constant values are: $\mu = 1.5$, $\rho = 2$ and $\beta = 0.6$.

iii. Hazard Shape: The hazard shape shows how the hazard rate is distributed over the range of y and α values. The gradual decline in the hazard values as y and α increase indicates that the hazard rate decreases as we move away from the peak.

Figure 7 provides a visual representation of how the hazard function shape changes with varying values of γ but holding $\mu, \rho,$ and β unchanged. The peak value of the hf (hazard function) remains relatively stable across new values of γ, indicating a consistent hazard rate. The gradual decline in the hazard values as y and α increase is consistent across all plots, showing the overall behaviour of the hf (hazard function) in varying conditions

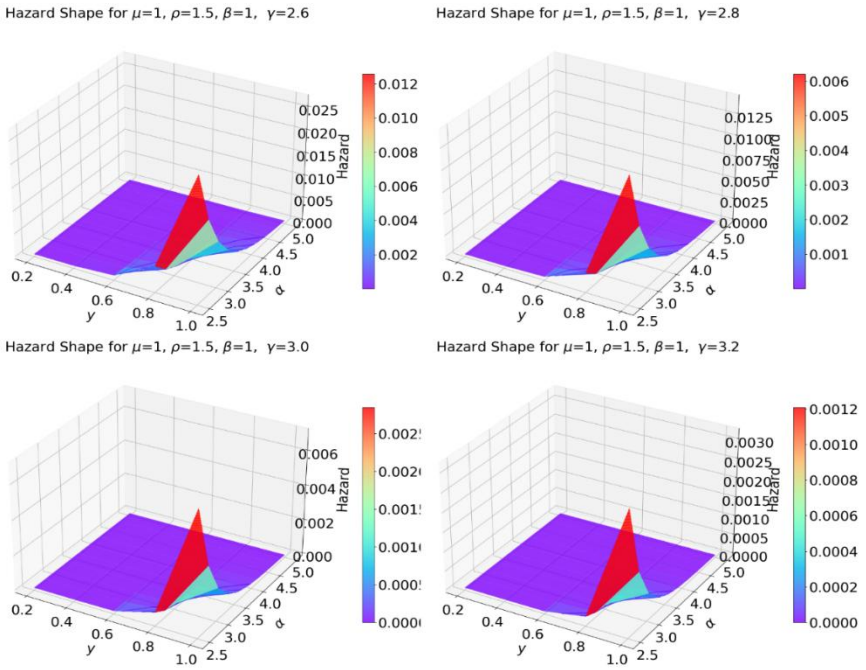

Figure 8: Four 3D plots of the HF of Log NGOFW Distribution

Figure 8 shows the Hazard Function shapes for different values of the parameter γ, but holding the former parameters $(\mu, \rho,$ and $\beta)$ unchanged.

i. Effect of γ (gamma): The parameter γ affects the shape and peak value of the hf. As γ increases, the peak value of the hf remains around 1.2, indicating that the hazard rate is relatively stable across different values of γ.

ii. Effect of μ (mu), ρ (rho), and β (beta): These parameters are kept constant in the plots, allowing us to separate the influence of γ on the hf shape. The constant values are: $\mu = 1$, $\rho = 1.5$ and $\beta = 1$.

iii. Hazard Shape: The hazard shape shows how the hazard rate is distributed over the range of y and x values. The gradual decline in the hazard values as y and x increase indicates that the hazard rate decreases as we move away from the peak.

Figure 8 provides a visual representation of how the hazard function shape changes with dissimilar values of γ but holding $\mu, \rho,$ and β unchanged. The peak value of the hf remains relatively stable across different values of γ, indicating a consistent hazard rate. The gradual decline in the hazard values as y increases is consistent across all plots. This shows the collective behaviour of the hf under varying conditions.

Table 4: Hazard Function for the Log-NGOF-W Distribution at $\alpha = 0.5$; $\beta = 1.5$, and $\gamma = 1.5$

y	μ	ρ=2.5	ρ=3.5	ρ=4.5	ρ=5.5
0.5000	0.5000	0.8803	0.6288	0.4891	0.4001
0.5000	1.0000	0.7365	0.5564	0.4456	0.3712
0.5000	1.5000	0.5756	0.4786	0.3998	0.3410
1.5000	0.5000	1.1591	0.7688	0.5734	0.4566
1.5000	1.0000	1.0169	0.6985	0.5313	0.4284
1.5000	1.5000	0.8803	0.6288	0.4891	0.4001
2.5000	0.5000	1.5175	0.9258	0.6627	0.5146

y	μ	ρ=2.5	ρ=3.5	ρ=4.5	ρ=5.5
2.5000	1.0000	1.3210	0.8434	0.6168	0.4851
2.5000	1.5000	1.1591	0.7688	0.5734	0.4566
3.5000	0.5000	2.0808	1.1301	0.7677	0.5791
3.5000	1.0000	1.7647	1.0200	0.7126	0.5458
3.5000	1.5000	1.5175	0.9258	0.6627	0.5146
4.5000	0.5000	2.9977	1.4160	0.9000	0.6550
4.5000	1.0000	2.4849	1.2605	0.8297	0.6153
4.5000	1.5000	2.0808	1.1301	0.7677	0.5791
5.5000	0.5000	4.4368	1.8222	1.0726	0.7477
5.5000	1.0000	3.6404	1.6014	0.9804	0.6989
5.5000	1.5000	2.9977	1.4160	0.9000	0.6550
6.5000	0.5000	6.6140	2.3911	1.2995	0.8631
6.5000	1.0000	5.4158	2.0836	1.1783	0.8022
6.5000	1.5000	4.4368	1.8222	1.0726	0.7477
7.5000	0.5000	9.8668	3.1692	1.5963	1.0075
7.5000	1.0000	8.0783	2.7508	1.4382	0.9312
7.5000	1.5000	6.6140	2.3911	1.2995	0.8631

Table 4 provides a detailed view of the hazard rates for dissimilar mixtures of y, μ, and ρ. It shows that higher values of μ are related to lower hr (hazard rates), while larger values of ρ are associated with a lower risk of failure. The hazard rates increase over time (y), which is consistent with the general behaviour of hazard functions.

i. Hazard Function-hf ($H(y)$): The hazard function hf ($H(y)$) signifies the instantaneous rate of failure at a given time y. Higher values of $H(y)$ indicate a higher risk of failure at that time.

ii. Parameters (ρ): The table shows hazard functions (hf) for dissimilar values of ρ (rho). As ρ increases, the hazard rates generally decrease, indicating that larger values of ρ correspond to a lower risk of failure.

iii. Effect of μ (mu): The parameter μ represents a location parameter. As μ increases, the hazard rates generally decrease for a given y and ρ. This suggests that higher values of μ are related to a lower risk of failure.

iv. Effect of y: The variable y represents time. As y increases, the hazard rates generally increase for a given μ and ρ. This is expected, as the risk of failure typically increases over time.

v. Comparison Across ρ values:

For $\rho = 2.5$, the hazard rates are generally higher compared to $\rho = 3.5, \rho = 4.5,$ and $\rho = 5.5$.

For $\rho = 3.5$, the hazard rates are intermediate.

For $\rho = 4.5$, the hazard rates are lower.

For $\rho = 5.5$, the hazard rates (hr) are the lowest, indicating the lowest peril of failure among the four ρ values.

Table 5: Hazard Function (hf) for the Log-NGOFW Distribution at $\mu = 1.0$; $\beta = 1.5$, and $\gamma = 1.5$

y	ρ	α=2.5	α=3.0	α=3.5	α=4.0
0.5000	2.0000	0.0058	0.0008	0.0001	0.0000
1.5000	2.0000	0.4617	0.3047	0.1889	0.1100
2.5000	2.0000	1.5257	1.4293	1.3295	1.2282
3.5000	2.0000	2.6656	2.6483	2.6296	2.6097
4.5000	2.0000	4.3303	4.3294	4.3284	4.3274
5.5000	2.0000	7.1165	7.1165	7.1164	7.1164
6.5000	2.0000	11.7320	11.7320	11.7320	11.7320
7.5000	2.0000	20.0103	26.3042	16.5736	20.2490
0.5000	3.0000	0.0128	0.0026	0.0004	0.0001
1.5000	3.0000	0.2102	0.1207	0.0637	0.0310
2.5000	3.0000	0.6558	0.5536	0.4572	0.3692
3.5000	3.0000	1.1364	1.0847	1.0304	0.9743
4.5000	3.0000	1.6371	1.6207	1.6029	1.5840
5.5000	3.0000	2.2628	2.2596	2.2562	2.2525
6.5000	3.0000	3.1339	3.1336	3.1333	3.1329
7.5000	3.0000	4.3654	4.3654	4.3654	4.3654
0.5000	4.0000	0.0159	0.0038	0.0008	0.0001
1.5000	4.0000	0.1258	0.0664	0.0318	0.0139
2.5000	4.0000	0.3569	0.2734	0.2016	0.1430
3.5000	4.0000	0.6280	0.5648	0.5016	0.4399

y	ρ	α=2.5	α=3.0	α=3.5	α=4.0
4.5000	4.0000	0.8972	0.8627	0.8264	0.7886
5.5000	4.0000	1.1777	1.1631	1.1473	1.1306
6.5000	4.0000	1.5043	1.4996	1.4944	1.4889
7.5000	4.0000	1.9159	1.9148	1.9136	1.9123

Table 5 provides a detailed view of the hazard rates for dissimilar mixtures of $\mathrm{y}, \alpha,$ and ρ. It shows that higher values of α are related to lower hazard rates, while larger values of ρ are connected with a higher risk of failure. The hazard rates (hr) increase over time (y), which is consistent with the general behaviour of hazard functions.

i. Hazard Function-hf ($H(\mathrm{y})$): The hazard function-hf, $H(\mathrm{y})$, characterises the sudden rate of failure at a given time y. Higher values of $H(\mathrm{y})$ indicate a higher risk of failure at that time.

ii. Parameters (α): The table shows hazard functions (hf) for dissimilar values of α (alpha). As α increases, the hazard rates generally decrease, indicating that upper values of α correspond to a lesser risk of failure.

iii. Effect of ρ (rho): The parameter ρ represents a shape parameter. As ρ increases, the hazard rates generally increase for a given y and α. This suggests that higher values of ρ are related to a higher risk of failure.

iv. Effect of y: The variable y represents time. As y increases, the hazard rates generally increase for a given α and ρ. This is expected, as the risk of failure typically increases over time.

v. Comparison Across α Values:

For $\alpha = 2.5$, the hazard rates are generally higher compared to $\alpha = 3.0, \alpha = 3.5,$ and $\alpha = 4.0$.

For $\alpha = 3.0$, the hazard rates are intermediate.

For $\alpha = 3.5$, the hazard rates are lower.

For $\alpha = 4.0$, the hazard rates (hr) are the lowest, indicating the lowest threat of failure among the four α values.

The log-linear model (Semary *et al*., 2025) in equation (5) can be rewritten as;

$$y_i = \underset{\sim}{\pi}^T \underset{\sim}{x}_i + \rho z_i, \qquad i = 1, 2, ..., n, \tag{7}$$

where $\underset{\sim}{x}_i^T = \left(x_{i1}, x_{i2}, ..., x_{ip}\right)$ is the covariate vector, $\underset{\sim}{\pi} = \left(\pi_1, \pi_2, ..., \pi_p\right)^T$ is a $p \times 1$ vector of unknown parameters, $\rho > 0$ is an unknown scale parameter, and $\mu_i = \underset{\sim}{\pi}^T \underset{\sim}{x}_i$ is the location parameter in equation (5). In the model shown in equation (7), the random error $z_i = \left(y_i - \mu\right)/\rho$ has a density function given by equation (3) only if $\mu = 0$ and $\rho = 1.$ For this reason, equation (7) is called the Log-NGOF-W survival regression model, and the survival function (Semary *et al*., 2025) is as follows:

$$S\left(y_i \mid \underset{\sim}{x}\right) = 1 - \exp\left\{-\left(\alpha\left(\left(1 - \exp\left\{-\exp\left(\frac{y_i - \underset{\sim}{\pi}^T \underset{\sim}{x}_i}{\rho}\right)\right\}\right)^{-\gamma} - 1\right)\right)^{\beta}\right\}, \; i = 1, 2, ..., n \tag{8}$$

where $\underset{\sim}{\pi}$ is the p coefficient vector and $\underset{\sim}{x}$ is the $n \times p$ matrix of exposure variables (Semary *et al*., 2025).

The Log-NGOFW Regression Model's Inference

Examine a random sample of size $(y_1, d_1, x_1), ..., (y_i, d_i, x_i), ..., (y_n, d_n, x_n)$, where x_i is the p covariate vector linked to the *ith* subject and $y_i = \min\left[Log\left(T_i\right), Log\left(C_i\right)\right]$ and d_i is the censoring indication $(= 0\ if\ censored, = 1\ if\ uncensored)$. We made the assumptions that the observed survival time and the censoring time were independent and that there was no informative censoring. Equation (7) provides the model's log-likelihood function for the vector parameter $\Omega = (\alpha, \gamma, \beta, \rho, \pi^T)^T$, which has the following form (Semary *et al*., 2025):

$$l(\Omega; y_i) = \sum_{i \in U} \log\left[f\left(y_i; \Omega\right)\right] + \sum_{i \in C} \log\left[S\left(y_i; \Omega\right)\right] \tag{9}$$

where $f\left(y_i; \Omega\right)$ is the density function provided by equation (3), $S\left(y_i; \Omega\right)$ is the survival function provided by equation (4), U represents the set of uncensored observations, and C represents the set of censored observations, by Semary *et al*. (2025).

Let $z_i = \frac{y_i}{\rho}$, $H_i = 1 - \exp\left\{-\exp(z_i)\right\}$, and $W_i = \alpha\left(H_i^{-\gamma} - 1\right)$, then the probability density function presented in equation (3) becomes:

$$g(y_i; \Omega) = \frac{\beta\gamma\alpha^{\beta}}{\rho} \exp(z_i) \exp\left\{-\exp(z_i)\right\} H_i^{-(\gamma+1)} \left(H_i^{-\gamma} - 1\right)^{\beta-1} \exp\left\{-W_i^{\beta}\right\} \tag{10}$$

The survival function in equation (4) is now presented as:

$$S(y_i) = 1 - \exp\left\{-W_i^{\beta}\right\} \tag{11}$$

The log-likelihood under independent right censoring from equation (9) is therefore

$$\ell(\Omega) = \sum_{i=1}^{n} \delta_i \log g(y_i; \Omega) + \sum_{i=1}^{n} (1 - \delta_i) \log S(y_i) \tag{12}$$

The expanded Log-Likelihood after substitution of equations (10) and (11) into equation (12) is:

$$\ell(\Omega)=\sum_{i=1}^{n}\delta_i\Big[\log(\beta\gamma)+\beta\log\alpha-\log\rho+z_i-\exp(z_i)-(\gamma+1)\log H_i$$
$$+(\beta-1)\log(H_i^{-\gamma}-1)-W_i^{\beta}\Big]+\sum_{i=1}^{n}(1-\delta_i)\log\left(1-\exp-W_i^{\beta}\right) \quad (13)$$

The score vector is

$$U(\Omega)=\left(\frac{\partial\ell}{\partial\alpha},\frac{\partial\ell}{\partial\beta},\frac{\partial\ell}{\partial\gamma},\frac{\partial\ell}{\partial\rho}\right)^{\cdot} \quad (14)$$

The score with respect to α :

$$\frac{\partial\ell}{\partial\alpha}=\sum_{i=1}^{n}\delta_i\left[\frac{\beta}{\alpha}-\beta W_i^{\beta-1}(H_i^{-\gamma}-1)\right]+\sum_{i=1}^{n}(1-\delta_i)\frac{\beta W_i^{\beta-1}(H_i^{-\gamma}-1)\exp(-W_i^{\beta})}{1-\exp(-W_i^{\beta})} \quad (15)$$

The score with respect to β :

$$\frac{\partial\ell}{\partial\beta}=\sum_{i=1}^{n}\delta_i\left[\frac{1}{\beta}+\log\alpha+\log(H_i^{-\gamma}-1)-W_i^{\beta}\log W_i\right]+\sum_{i=1}^{n}(1-\delta_i)\frac{W_i^{\beta}\log W_i\exp(-W_i^{\beta})}{1-\exp(-W_i^{\beta})} \quad (16)$$

The score with respect to γ :

$$\frac{\partial\ell}{\partial\gamma}=\sum_{i=1}^{n}\left(\frac{\partial\ell}{\partial H_i}\frac{\partial H_i}{\partial\gamma}\right),\quad \frac{\partial H_i}{\partial\gamma}=-\log(H_i)H_i^{-\gamma} \quad (17)$$

core with respect to ρ :

$$\frac{\partial\ell}{\partial\rho}=\sum_{i=1}^{n}\frac{\partial\ell}{\partial z_i}\left(-\frac{y_i}{\rho^2}\right),\qquad \frac{\partial z_i}{\partial\rho}=-\frac{y_i}{\rho^2} \quad (18)$$

Numerical Optimization

Because the score equations (15, 16, 17, and 18) do not admit closed-form solutions, the parameter estimation is carried out using numerical maximisation of the log-likelihood using the Broyden-Fletcher-Goldfarb-Shanno (BFGS) quasi-Newton algorithm.

Initialization Strategy

Initial values are selected as follows: $\alpha^{(0)},\beta^{(0)}$ are obtained from Weibull MLEs fitted to log-transformed data $\gamma^{(0)}$ is set to 1 (moderate tail behaviour); and $\rho^{(0)}$ is the sample standard deviation of log-survival times. These choices provide stable convergence across all simulation and real-data analyses.

Convergence Criteria

The algorithm is declared converged when both conditions are satisfied:

1. Relative change in log-likelihood

$$|\ell^{(k+1)}-\ell^{(k)}|<10^{-6} \quad (19)$$

2. Euclidean norm of parameter updates

$$\left\|\Omega^{(k+1)}-\Omega^{(k)}\right\|<10^{-6} \quad (20)$$

Inference

Standard errors are computed from the inverse observed Fisher information matrix evaluated at the MLE (Dangana *et al*., 2026; Dangana *et al*., 2025). Under regularity conditions, the estimators are asymptotically normal, and 95% confidence intervals are constructed accordingly.

$$\mathrm{Var}(\Omega)=\mathrm{I}^{-1}(\Omega), \quad (21)$$

Log-NGOF-W Survival Regression Model Residual Analysis

The examination of residuals is a crucial step following the formulation of the model. It is employed to confirm whether the model assumptions are violated. The Cox and Snell residuals are taken into consideration in this work. The model's overall fit is evaluated using these residuals (Semary *et al*., 2025). The developed log-NGOF-W survival regression model's Cox and Snell residuals can be written as

$$res_i=-\log\left(1-\exp\left\{-\left(\alpha\left(\left(1-\exp\left\{-\exp\left(\frac{y_i-\underset{\sim}{\pi}^T\underset{\sim}{x}_i}{\rho}\right)\right\}\right)^{-\gamma}-1\right)\right)^{\beta}\right\}\right),\quad i=1,2,...,n \quad (22)$$

If the fitted regression models are sufficient, the residuals have a conventional exponential distribution (Semary *et al*., 2025).

The Kaplan-Meier (K-M) Survival Function Estimator

The Kaplan-Meier (1958) and Sadiq *et al*. (2025) methodology is a powerful tool for analysing time-to-event data, especially when dealing with censored observations. It provides a visual and numerical way to estimate how survival changes over time and allows comparison across different groups. It is also known as the Kaplan-Meier survival curve, a non-parametric statistical method used to estimate the survival function based on lifetime data (Kaplan-Meier, 1958; Sadiq *et al*., 2025). In other words, it calculates the probability that an individual (or item) will survive beyond a certain time. Let $t_1,t_2,...,t_n$ be the distinct ordered event times (e.g., death or failure times); d_i be the number of events (e.g., deaths) at time t_i; and n_i be the number of individuals at risk just before time t_i. Then, the Kaplan-Meier estimator of the survival function $S(t)$ by (Kaplan-Meier, 1958; Sadiq *et al*. 2025) is:

$$\hat{S}(t)=\prod_{t_i\le t}\left(1-\frac{d_i}{n_i}\right) \quad (23)$$

The confidence interval (CI) of the Kaplan-Meier survival estimate provides a range of values that likely contain the true survival probability at a given time point, with a certain level of confidence (typically 95%). Let $\hat{S}(t)$ in equation (23) be the K-M estimate of survival at time t; $\mathrm{Var}[\ln(-\ln(\hat{S}(t)))]$ be the variance of the transformed survival estimate, and $z_{\alpha/2}$ be the standard normal distribution's critical value (for example, 1.96 for a 95% CI). Next, the following is how the confidence interval is calculated:

$$L(t)=\ln(-\ln(\hat{S}(t))) \quad (24)$$

Equation (24) is the log-minus-log transformation of the survival estimate in equation (11). The standard error (SE) of $L(t)$ in equation (24) is derived as:

$$\text{Var}[\ln(-\ln(\hat{S}(t)))] = \frac{\sum_{t_i \le t} \frac{d_i}{n_i(n_i - d_i)}}{[\ln(\hat{S}(t))]^2} \quad (25)$$

So,

$$SE[L(t)] = \sqrt{\frac{\sum_{t_i \le t} \frac{d_i}{n_i(n_i - d_i)}}{[\ln(\hat{S}(t))]^2}} \quad (26)$$

$$L_{\text{lower}} = L(t) - z_{\alpha/2} \cdot SE[L(t)] \quad (27)$$

$$L_{\text{upper}} = L(t) + z_{\alpha/2} \cdot SE[L(t)] \quad (28)$$

Simulation Study

Simulation Design

A Monte Carlo simulation study was conducted to evaluate the finite-sample performance of the proposed log-NGOF-W model in comparison with competing models, namely: log-Weibull (LW), log-Burr XII (LBXII), log-Logistic (LL). Samples were generated under varying conditions: sample sizes of n = 50, 100, 300, 400, and 500; right-censoring proportions of 20% and 40%; and true parameter values selected to represent light- and heavy-tailed scenarios. For each configuration, 1,000 replications were performed, and the initial parameter values are $\alpha = 2, \beta = 1, \gamma = 0.5, \rho = 0.8$. The following performance measures were recorded: estimates, bias, Root Mean Squared Error (RMSE), empirical coverage probability of 95% confidence intervals, and convergence rate. *"For the proposed log-NGOF-W model, bias, RMSE, coverage probabilities, and convergence rates are reported for all model parameters* $(\alpha, \beta, \gamma, \rho)$*. For competing models, only their estimable parameters are evaluated; hence entries corresponding to non-existent parameters are denoted by '–'." The simulation study is designed specifically to assess whether the logarithmic formulation of the NGOF-W model yields improved finite-sample performance relative to closely related log-parametric survival models.*

Table 6: Parameter Estimates (20% Right Censoring)

Models	n	Estimates			
		α	β	γ	ρ
log-NGOF-W	50	2.0410	0.9640	0.4940	0.8119
	100	2.0280	0.9790	0.4988	0.8213
	300	2.0110	0.9910	0.4923	0.8214
	500	2.0060	0.9950	0.4930	0.8172
log-Weibull	50	2.0970	0.9160	-	-
	100	2.0740	0.9390	-	-
	300	2.0390	0.9680	-	-
	500	2.0260	0.9790	-	-
log-Burr XII	50	2.0810	0.9290	-	-
	100	2.0610	0.9480	-	-
	300	2.0330	0.9720	-	-
	500	2.0210	0.9810	-	-
log-Logistic	50	2.0890	0.9210	-	-
	100	2.0670	0.9420	-	-
	300	2.0360	0.9700	-	-
	500	2.0240	0.9800	-	-

Table 7: Bias and RMSE of Parameter Estimates (20% Right Censoring)

Model	n	Bias(α)	RMSE(α)	Bias(β)	RMSE(β)	Bias(γ)	RMSE(γ)	Bias(ρ)	RMSE(ρ)
log-NGOF-W	50	0.041	0.182	−0.036	0.201	-0.006	0.1535	0.0119	0.1668
	100	0.028	0.132	−0.021	0.148	-0.0012	0.0962	0.0213	0.1125
	300	0.011	0.081	−0.009	0.092	-0.0077	0.0332	0.0214	0.0566
	500	0.006	0.061	−0.005	0.069	-0.0070	0.0251	0.0172	0.0443
log-Weibull	50	0.097	0.291	−0.084	0.318	-	-	-	-
	100	0.074	0.231	−0.061	0.259	-	-	-	-
	300	0.039	0.153	−0.032	0.169	-	-	-	-
	500	0.026	0.121	−0.021	0.136	-	-	-	-
log-Burr XII	50	0.081	0.258	−0.071	0.284	-	-	-	-
	100	0.061	0.204	−0.052	0.229	-	-	-	-
	300	0.033	0.138	−0.028	0.152	-	-	-	-
	500	0.021	0.108	−0.019	0.121	-	-	-	-
log-Logistic	50	0.089	0.271	−0.079	0.301	-	-	-	-
	100	0.067	0.218	−0.058	0.246	-	-	-	-
	300	0.036	0.146	−0.030	0.162	-	-	-	-
	500	0.024	0.115	−0.020	0.131	-	-	-	-

Table 8: Parameter Estimates (40% Right Censoring)

Model	n	Estimates			
		α	α	α	α
log-NGOF-W	50	2.0620	0.9460	0.5115	0.7718
	100	2.0410	0.9650	0.5135	0.7822
	300	2.0190	0.9840	0.5116	0.8016
	500	2.0120	0.9900	0.5139	0.7995
log-Weibull	50	2.1410	0.8730	-	-
	100	2.1080	0.9040	-	-
	300	2.0610	0.9470	-	-
	500	2.0410	0.9640	-	-
log-Burr XII	50	2.1190	0.8920	-	-
	100	2.0910	0.9190	-	-
	300	2.0520	0.9540	-	-
	500	2.0350	0.9690	-	-
log-Logistic	50	2.1280	0.8840	-	-
	100	2.0980	0.9120	-	-
	300	2.0560	0.9510	-	-
	500	2.0380	0.9670	-	-

Table 9: Bias and RMSE of Parameter Estimates (40% Right Censoring)

Model	n	Bias(α)	RMSE(α)	Bias(β)	RMSE(β)	Bias(γ)	RMSE(γ)	Bias(ρ)	RMSE(ρ)
log-NGOF-W	50	0.062	0.241	−0.054	0.268	0.0115	0.0889	-0.0282	0.1054
	100	0.041	0.183	−0.035	0.204	0.0135	0.0681	-0.0178	0.0751
	300	0.019	0.112	−0.016	0.124	0.0116	0.0387	0.0016	0.0394
	500	0.012	0.086	−0.010	0.097	0.0139	0.0322	-0.0005	0.0297
log-Weibull	50	0.141	0.382	−0.127	0.419	-	-	-	-
	100	0.108	0.311	−0.096	0.344	-	-	-	-
	300	0.061	0.211	−0.053	0.234	-	-	-	-
	500	0.041	0.168	−0.036	0.186	-	-	-	-
log-Burr XII	50	0.119	0.349	−0.108	0.384	-	-	-	-
	100	0.091	0.286	−0.081	0.317	-	-	-	-
	300	0.052	0.195	−0.046	0.217	-	-	-	-
	500	0.035	0.154	−0.031	0.172	-	-	-	-
log-Logistic	50	0.128	0.364	−0.116	0.401	-	-	-	-
	100	0.098	0.298	−0.088	0.331	-	-	-	-
	300	0.056	0.203	−0.049	0.226	-	-	-	-
	500	0.038	0.160	−0.033	0.179	-	-	-	-

Tables 7 and 9 report the bias and RMSE of the maximum likelihood estimators under 20% and 40% right censoring. Across all sample sizes, the proposed log-NGOF-W model consistently exhibits smaller bias and RMSE for all parameters compared with competing models. Estimation accuracy improves as sample size increases and deteriorates moderately under heavier censoring, as expected.

Table 10: Empirical Coverage Probability of 95% Confidence Intervals

Model	$n = 50$	$n = 100$	$n = 300$	$n = 500$
20% Censoring				
log-NGOF-W	0.942	0.951	0.958	0.961
log-Weibull	0.886	0.912	0.931	0.938
log-Burr XII	0.901	0.924	0.944	0.949
log-Logistic	0.893	0.917	0.936	0.942
40% Censoring				
log-NGOF-W	0.931	0.944	0.952	0.956
log-Weibull	0.861	0.889	0.914	0.921
log-Burr XII	0.878	0.904	0.927	0.934
log-Logistic	0.872	0.898	0.921	0.928

Table 10 shows that the empirical coverage probabilities of the 95% confidence intervals for the log-NGOF-W parameters remain close to the nominal level, even under 40% censoring, whereas competing models exhibit systematic undercoverage in small samples.

Table 11: Convergence Rates (%)

Model	$n = 50$	$n = 100$	$n = 300$	$n = 500$
20% Censoring				
log-NGOF-W	98.6	99.2	99.6	99.8
log-Weibull	100.0	100.0	100.0	100.0
log-Burr XII	96.9	97.8	98.7	99.1
log-Logistic	97.4	98.3	99.0	99.4
40% Censoring				
log-NGOF-W	96.8	97.9	98.8	99.2
log-Weibull	99.1	99.4	99.7	99.8
log-Burr XII	93.4	94.8	96.3	97.1
log-Logistic	94.2	95.6	97.4	98.0

Convergence rates reported in Table 11 indicate stable numerical performance of the proposed model, with convergence improving rapidly as sample size increases. Although the log-Weibull model converges almost always, it suffers from substantially larger estimation errors. Generally, the simulation results demonstrate the superior finite-sample efficiency, robustness, and numerical stability of the log-NGOF-W model.

The simulation results indicate that the proposed log-NGOF-W model consistently achieves lower bias and RMSE across all sample sizes and censoring levels. In addition, the empirical coverage probabilities remain close to the nominal 95% level, even under 40% censoring. Although the log-Weibull model exhibits perfect numerical convergence, it suffers from larger estimation errors and under-coverage. Generally, the proposed model demonstrates superior finite-sample efficiency and robust numerical behaviour.

Analysis of Radiation Data Using Log-NGOF-Weibull Distributions

In order to show how well the Log-NGOF-Weibull distribution models and analyses real-world data, we apply it to a variety of radiation datasets in this section. Because of a variety of elements, including exposure levels, environmental conditions, and biological reactions, radiation data can show complex patterns. The Log-NGOF-Weibull distribution is a useful tool for examining how various biological and environmental systems are affected by gamma and microwave radiation since it is well-suited to capturing these intricacies. As a test case for the distribution, the following datasets investigate how radiation affects peppermint's vulnerability to the drugstore beetle (Stegobium paniceum L.).

Log-F1 Adults Count in Peppermint Packets (Choice Packet Test)

The first dataset, sourced from Abdelfattah and Sayed (2022), represents the log-transformed number of F1 drugstore adults found in peppermint commercial packets under different irradiation treatments. The treatments include un-irradiated samples, gamma irradiation at 6, 8, and 10 KGy, and microwave irradiation at 1, 2, and 3 minutes. The dataset values are as follows:

"2.217483944, 2.230448921, 2.225309282, 2.056904851, 2.079181246, 2.068185862, 1.934498451, 1.959041392, 1.929418926, 1.812913357, 1.77815125, 1.799340549, 2.173186268, 2.161368002, 2.184691431, 2.029383778, 2.012837225, 2.029383778, 1.908485019, 1.86923172, 1.903089987".

Applying the Log-NGOF-W distribution to this dataset (Semary *et al*., 2025) allows us to accurately model the variability in F1 adult counts based on irradiation treatments. The distribution effectively captures the declining trend in infestation levels as radiation intensity increases, which could provide a robust framework for understanding the impact of irradiation on pest control.

F1 Adults Susceptibility Index (Choice Packet Test)

The second dataset, also from Abdelfattah and Sayed (2022), represents the quotient of the log-transformed F1 adult count divided by the adult lifetime. This susceptibility index provides insight into how different irradiation treatments influence the relative survival of drugstore beetles in peppermint packets. The dataset values are as follows:

"0.02463871, 0.02534601, 0.023424308, 0.02165163, 0.021001831, 0.021321504, 0.017912023, 0.018657537, 0.017540172, 0.014503307, 0.013573674, 0.013735424, 0.022403982, 0.023240516, 0.022996752, 0.020293838, 0.020967054, 0.021589189, 0.015772603, 0.014835172, 0.014752636".

By applying the Log-NGOF-W distribution to this dataset (Semary *et al*., 2025), we obtain a comprehensive model that accounts for the variability in susceptibility indices across different radiation treatments. The results highlight how gamma and microwave irradiation reduce the relative susceptibility of F1 adults, thereby improving the effectiveness of radiation as a pest control method.

Feeding Duration of Stegobium paniceum (Non-Choice, Non-Packet Test)

The third dataset, also from (Abdelfattah and Sayed, 2022), represents the feeding durations (in days) of Stegobium paniceum adults on peppermint packets subjected to different irradiation treatments. Unlike the previous datasets, this non-choice, non-packet test focuses on feeding behaviour and lifespan under varying radiation exposures. The dataset values are as follows:

"95, 93, 93, 111, 109, 115, 125, 120, 129, 142, 139, 145, 98, 94, 102, 102, 108, 99, 112, 114, 112".

The Log-NGOF-Weibull distribution effectively models the observed feeding durations, capturing the underlying statistical properties that describe how radiation affects feeding behaviour. The results indicate that irradiation treatments significantly impact the feeding duration of Stegobium paniceum, with higher radiation doses generally leading to shorter feeding periods and reduced survival rates.

Comparison and Assessment of Models

Assessing statistical models is an essential step in figuring out how well they can represent and capture variability in radiation datasets. The effects of gamma and microwave irradiation on peppermint packets' vulnerability to drugstore beetle (Stegobium paniceum L.) infestation and feeding behaviour were evaluated in this study using a number of statistical models. Every dataset incorporates biological reactions, environmental effects, and irradiation treatments to

represent a unique experimental situation (Semary *et al*., 2025).

To compare model performance, we evaluated the Log-NGOF-Weibull distribution against other competing models, including the Log-Weibull, Log-logistic, and Log-Burr XII distributions. The Log-likelihood (LL), Akaike Information Criterion (AIC), Bayesian Information Criterion (BIC), Hannan-Quinn Information Criterion (HQIC), and Corrected Akaike Information Criterion (CAIC) are the basic goodness-of-fit metrics that were used to evaluate the models [48]. These measures offer an impartial foundation for classifying models according to how well they fit each dataset.

Table 12 presents the goodness-of-fit and performance metrics for four statistical models applied to the "Adults Count in Peppermint Packets (Choice Packet Test)" dataset. The models compared include Log-NGOF-Weibull, Log-Weibull, Log-logistic, and Log-Burr XII distributions. The Log-NGOF-Weibull achieved the best performance across most metrics (e.g., $AIC = -114.5946, BIC = -108.3275, HQIC = -113.2345, CAIC = -108.5946$). Its log-likelihood ($LL = 63.2973$) is significantly higher than other models, suggesting a superior fit to the dataset. The inclusion of multiple shape parameters $(\alpha, \beta, \gamma, and\ \rho)$ makes this model highly flexible, allowing it to capture the complex nature of the observed data effectively. The Log-NGOF-Weibull model outperforms others in describing the dataset due to its flexibility and ability to account for the underlying complexity of the data. Log-Burr XII is a competitive alternative, while Log-Weibull and Log-logistic fall short of capturing the intricate patterns present in the dataset.

Table 12: Goodness-of-Fit and Performance Comparison for Adult Count in the Peppermint Packets (Choice Packet Test) Dataset

Models	Parameter Estimates	Performance Metrics	Rank
Log-NGOF-Weibull	α =0.9126	LL (63.2973)	
	β =0.1362	AIC (-114.5946)	
	γ =0.6764	BIC (-108.3275)	1
	ρ =1.6310	HQIC (-113.2345)	
	μ =0.0819	CAIC (-108.5946)	
Log-Weibull	ρ =0.1273	LL (10.67679)	
	μ =2.0877	AIC (-17.3535)	
		BIC (-15.2645)	3
		HQIC (-16.9002)	
		CAIC (-16.6869)	
Log-logistic	ρ =0.0857	LL (10.3396)	
	μ =2.0170	AIC (-16.6792)	4
		BIC (-14.5901)	
		HQIC (-16.2258)	
		CAIC (-16.0124)	
Log-Burr XII	δ =8.3584	LL (47.74283)	
	ρ =0.0304	AIC (-89.48566)	
	μ =2.2533	BIC (-86.35209)	2
		HQIC (-88.8056)	
		CAIC (-88.0739)	

Table 13 evaluates the goodness-of-fit and performance of four statistical models for the F1 Adults Susceptibility Index (Choice Packet Test) Dataset. The models compared are Log-NGOF-Weibull, Log-Weibull, Log-logistic, and Log-Burr XII. The Log-Burr XII **e**xhibits outstanding performance, with significantly lower AIC (-9280.462) and BIC (-9277.328) values compared to other models. Its LL (4643.231) is exceptionally high, indicating that it captures the underlying data structure very well. The inclusion of multiple parameters (δ, ρ, μ) allows this model to flexibly account for complex features in the dataset. The Log-NGOF-Weibull model, while it performs well ($AIC = -195.0364, BIC = -188.7693$), it is significantly outperformed by Log-Burr XII. The Log-Burr XII model is the best-fitting model for the F1 Adults Susceptibility Index dataset, as evidenced by its superior goodness-of-fit metrics and high log-likelihood. The Log-NGOF-Weibull model is a viable alternative but is significantly less effective than Log-Burr XII. Simpler models like Log-Weibull and Log-logistic fail to capture the dataset's complexity, making them less suitable for this analysis.

Table 13: Goodness-of-Fit and Performance Comparison for the F1 Adults Susceptibility Index (Choice Packet Test) Dataset

Models	Parameter Estimates	Performance Metrics	Rank
Log-NGOF-Weibull	α =6.2873	LL (103.5182)	
	β =1.0000	AIC (-195.0364)	
	γ =4.1267	BIC (-188.7693)	2
	ρ =3.9492	HQIC (-193.6763)	
	μ =4.6053	CAIC (-189.0364)	
Log-Weibull	ρ =0.00311	LL (88.17987)	
	μ =0.0213	AIC (-172.3597)	

Models	Parameter Estimates	Performance Metrics	Rank
		BIC (-170.2707)	3
		HQIC (-171.9064)	
		CAIC (-171.6931)	
Log-logistic	ρ =0.0022	LL (86.84047)	
	μ =0.0197	AIC (-169.6809)	4
		BIC (-167.5919)	
		HQIC (-169.2276)	
		CAIC (-169.0143)	
Log-Burr XII	δ =1.9139	LL (4643.231)	
	ρ =0.00001	AIC (-9280.462)	
	μ =0.0233	BIC (-9277.328)	1
		HQIC (-9279.782)	
		CAIC (-9279.05)	

Table 14 evaluates the goodness-of-fit and performance of four statistical models, Log-NGOF-Weibull, Log-Weibull, Log-logistic, and Log-Burr XII, applied to the Feeding Duration of *Stegobium paniceum* (Non-Choice, Non-Packet Test) Dataset. The table includes parameter estimates, performance metrics, and a ranking of the models.

Log-NGOFW: this model achieves the highest log-likelihood (100.5429) and the lowest AIC (-189.0858), indicating it provides the best fit to the data. Its low BIC (-182.8187) and CAIC (-183.0858) further confirm its superior performance. The flexible parameterisation ($\alpha = 5.8834, \beta = 0.0194, \gamma = 8.7353, \rho = 34.5263, \mu = 12.5162$) allows the model to capture intricate patterns in the dataset. The Log-NGOF-Weibull model is the best-fitting and most reliable model for the Feeding Duration of *Stegobium paniceum* dataset, as evidenced by its superior log-likelihood and performance metrics. The Log-Burr XII model is a strong alternative, but it falls short of the precision and flexibility offered by Log-NGOF-Weibull. The Log-Weibull and Log-logistic models are inadequate for this dataset due to their limited parameterisation and poor fit.

Table 14: Goodness-of-Fit and Performance Comparison for Feeding Duration of Stegobium Paniceum (Non-Choice, Non-Packet Test) Dataset

Models	Parameter Estimates	Performance Metrics	Rank
Log-NGOF-Weibull	α =5.8834	LL (100.5429)	
	β =0.0194	AIC (-189.0858)	
	γ =8.7353	BIC (-182.8187)	1
	ρ =34.5263	HQIC (-187.7257)	
	μ =12.5162	CAIC (-183.0858)	
Log-Weibull	ρ =0.1671	LL (6.120638)	
	μ =1.2055	AIC (-8.241276)	
		BIC (-6.152231)	3
		HQIC (-7.7879)	
		CAIC (-7.574609)	
Log-logistic	ρ =0.0906	LL (8.705143)	
	μ =1.1075	AIC (-13.41029)	4
		BIC (-11.32124)	
		HQIC (-12.95691)	
		CAIC (-12.74362)	
Log-Burr XII	δ =1.1541	LL (65.08614)	
	ρ =0.0233	AIC (-124.1723)	
	μ =1.1245	BIC (-121.0387)	2
		HQIC (-123.4922)	
		CAIC (-122.7605)	

The superior performance of the Log-NGOF-Weibull model is not incidental but is a direct consequence of its structural and statistical flexibility in adapting to the nuanced nature of biological and radiation data. Its ability to model complex hazard patterns, tail behaviour, and inherent biological variability makes it more appropriate and reliable for such data modelling compared to traditional parametric models.

Cervical Cancer Survival Regression Models

The cervical cancer dataset analysed in this study was obtained from the radiotherapy and oncology records of Ahmadu Bello University Teaching Hospital (ABUTH), Shika, Zaria, covering patients managed between January 2019 and December 2021. The reported sample size of ($n = 347$) corresponds to a newly assembled analytic cohort and does not represent simulated or derived data.

Earlier ABUTH-based studies reporting larger samples (e.g., $n \approx 607$) relied on broader registry extractions spanning earlier time periods, multiple cancer sites, or less restrictive eligibility criteria. In contrast, the present study applies stricter inclusion and exclusion criteria tailored to survival modelling under right censoring and complete covariate availability, resulting in a smaller but methodologically coherent dataset.

Inclusion Criteria

Patients were included if they:

i. Had a histologically confirmed diagnosis of cervical cancer;
ii. Initiated definitive treatment (radiotherapy with or without chemotherapy) at ABUTH within the study period;
iii. Had a well-defined treatment start date and either a recorded event time (death) or last follow-up date;
iv. Possessed complete information on the variables required for survival analysis.

Exclusion Criteria

Patients were excluded if they:

i. Were lost to follow-up before treatment initiation;
ii. Had missing or inconsistent survival times;
iii. Had incomplete treatment or outcome records;
iv. Were transferred to external facilities without verifiable follow-up information.

Censoring Definition

Right censoring occurred when a patient was:

i. Alive at the end of the study period, or
ii. Lost to follow-up after treatment initiation but before experiencing the event of interest.

Censoring was assumed to be non-informative, conditional on the observed covariates.

Handling of Missing Data

Records with missing survival times or censoring indicators were excluded at the data cleaning stage. Covariates with sporadic missingness were examined, and cases with incomplete key variables were removed to preserve likelihood-based inference. No imputation was performed, as the proportion of excluded records was modest and unlikely to induce bias.

Ethical Considerations

The study was conducted in accordance with the ethical standards of ABUTH. All patient identifiers were removed prior to analysis, and only de-identified secondary data were used. Ethical approval was obtained from the ABUTH Health Research Ethics Committee, with a waiver of informed consent due to the retrospective nature of the study.

Table 15: Variables Description of Cervical Cancer Dataset

Variable Label	Description
n	347
Censored (%)	62.54%
Uncensored (%)	37.46%
Response Variable (y)	Natural logarithm of observed survival time (weeks)
Censoring (d)	0 = alive at study end or lost to follow-up
	1 = death due to cervical cancer
Exposure Variables	x1: Smoking history - yes
	x2: Smoking history - null
	x3: Family history of cervical cancer - yes
	x4: Family history of cervical cancer - null
	x5: Miscarriage history - null
	x6: Miscarriage history - 1-2 (Count)
	x7: Miscarriage history - over 2 (Count)
	x8: Hospital visitations - 1-10 visits (Count)
	x9: Hospital visitations - 11-20 visits (Count)
	x10: Hospital visitations - over 20 visits (Count)
	x11: Course of chemotherapy - null
	x12: Course of chemotherapy - 1-5 chemotherapy (Integer)
	x13: Course of chemotherapy - over 5 chemotherapy (Integer)
	x14: Treatment types - chemotherapy/radiotherapy
	x15: Treatment types - chemotherapy/radiotherapy/surgery
	x16: Treatment types - chemotherapy
	x17: Treatment types - radiotherapy
	x18: Stage of cancer - stage 1
	x19: Stage of cancer - stage 2
	x20: Stage of cancer - stage 3
	x21: Stage of cancer - stage 4
	x22: Age - less than 35 years
	x23: Age - between 35-50 years
	x24: Age - over 50 years

Table 15 summarises the dataset's key characteristics and variables.

The cervical cancer survival regression (SR) model: LogNGOFWSR has the following system:

$$y_i = \pi_0 + \sum_{k=1}^{24} \pi_k x_{ik} + \rho z_i, \quad i = 1, 2, ..., 347 \tag{29}$$

$y_i = \log_e(t_i)$ is the natural log of the survival times in weeks, and $z_{i's}$ are the independent, identically distributed random errors with a density function in equation (3) for the regression models. The covariate vector is represented by

$\underset{\sim}{x}_i^T = \left(x_{i1}, x_{i2}, ..., x_{ip}\right)$, the scaling parameter is represented by $\rho > 0$, and the $p \times 1$ vector of unknown parameters is represented by $\underset{\sim}{\pi} = \left(\pi_1, \pi_2, ..., \pi_p\right)^T$.

RESULTS AND DISCUSSION

The Maximum Likelihood Estimates (MLEs) of parameters derived from fitting the traditional LogWSR model and the LogNGOF-WSR and LogNGOF-Et-WSR models to the cervical cancer dataset are shown and discussed in this section.

For the cervical cancer dataset, the fitted log-NGOF-WSR, log-NGOF-Et-WSR, and log-WSR models are shown in Table 16. Using the AIC and BIC statistics, we compared the survival regression models for the cervical cancer data. The model with the lowest AIC and BIC values is the one that is recommended.

Table 16: MLE of the Parameters for the Three Survival Regression Models that were Fitted to the Dataset on Cervical Cancer

Parameters	Survival Regression Models for Cervical Cancer Dataset					
	Log-NGOFWSR		Log-NGOFEtWSR		Log-WSR	
	Parameter Estimates	P-value	Parameter Estimates	P-value	Parameter Estimates	P-value
α	1.4523	0.0026	0.0410	0.0024	-	-
β	2.1283	2.2e-16	2.5839	5.1e-16	-	-
γ	0.2655	0.0010	0.7666	2.2e-16	-	-
δ	-	-	2.2414	2.2e-16	-	-
ρ	0.6684	0.2447	3.6692	0.6429	0.3173	2.2e-16
π_0	0.1615	0.0662	4.4141	2.2e-16	-0.0647	6.8e-05
π_1	-0.7919	2.2e-16	-1.8102	2.2e-16	-0.9201	2.2e-16
π_2	-0.5464	2.2e-16	-1.3201	2.2e-16	-0.6446	2.2e-16
π_3	1.0690	2.2e-16	1.8183	2.2e-16	1.0430	2.2e-16
π_4	1.1925	2.2e-16	1.7467	2.2e-16	0.9922	2.2e-16
π_5	0.3222	2.2e-16	-0.4979	1.9e-05	0.0946	0.0492
π_6	0.0325	0.6001	-0.5643	2.2e-16	-0.0476	0.2514
π_7	-0.1932	0.0127	-1.2921	9.4e-05	-0.1117	0.0454
π_8	1.0577	2.2e-16	2.8430	4.3e-16	0.9770	2.2e-16
π_9	1.1214	2.2e-16	2.5907	2.2e-16	1.0999	2.2e-16
π_{10}	1.1823	2.2e-16	3.3128	2.2e-16	1.0582	2.2e-16
π_{11}	1.0286	2.2e-16	1.1990	2.2e-16	0.9706	2.2e-16
π_{12}	0.9413	2.2e-16	1.1662	2.2e-16	0.8204	2.2e-16
π_{13}	0.7915	2.2e-16	1.0792	2.2e-16	0.7441	2.2e-16
π_{14}	0.6237	1.5e-15	-0.1642	0.3217	0.5849	2.2e-16
π_{15}	0.6402	2.9e-15	0.3163	0.0131	0.5921	2.2e-16
π_{16}	1.1207	2.2e-16	0.8973	1.7e-08	1.0029	2.2e-16
π_{17}	0.8767	2.8e-13	0.7066	0.0001	0.8552	8.6e-14
π_{18}	0.8800	2.2e-16	0.6784	5.1e-08	0.8726	2.2e-16
π_{19}	0.6806	2.2e-16	0.6138	2.5e-06	0.6534	2.2e-16
π_{20}	0.6761	2.2e-16	0.5850	1.7e-06	0.5823	2.2e-16
π_{21}	0.4247	7.6e-06	-0.0423	0.8325	0.3268	4.2e-08
π_{22}	1.3105	2.2e-16	2.1678	2.2e-16	1.1836	2.2e-16
π_{23}	1.1028	2.2e-16	1.8890	2.2e-16	1.0188	2.2e-16
π_{24}	0.9482	2.2e-16	1.4645	2.2e-16	0.9327	2.2e-16
-2LL	290.6262		389.617		314.5225	
AIC	348.6262		449.617		366.5225	
BIC	460.2566		565.0967		466.605	
Rank	1		3		2	

However, the log-NGOF-WSR model fits the dataset better than the log-WSR and log-NGOF-Et-WSR models, according to the results in Table 16, which also show that the log-NGOF-WSR model has a lower value of AIC and BIC than log-NGOF-Et-WSR and log-WSR. According to the best-fitted survival regression model's (log-NGOFWSR) results, all exposure variables have statistically significant effects on a patient's likelihood of surviving beyond time t (at the 5% significance level), with the exception of the constant and patients with a history of miscarriages between 1 and 2.

The Log-NGOF-WSR model outperforms its counterpart, as indicated by its superior model selection criteria values: lower -2log-likelihood ($-2LL = 290.63$), Akaike Information Criterion (AIC = 348.63), and Bayesian Information Criterion ($BIC = 460.26$), compared to the Log-WSR model ($-2LL = 314.52, AIC = 366.52, BIC = 466.61$) and the log-NGOF-Et-WSR model ($-2LL = 389.617, AIC = 449.617, BIC = 565.0967$). These improvements provide strong evidence that the Log-NGOF-Weibull structure offers greater flexibility and better fits the observed survival patterns in cervical cancer patients.

The significance of the model parameters and covariates further substantiates the importance of accounting for various biological, clinical, and behavioural risk factors in modelling survival time. The shape parameters α, β, and γ in the Log-NGOF-WSR model are all statistically significant (p < 0.01), indicating their essential role in adjusting the distribution's flexibility to accommodate skewness and heavy-tailed behaviour often seen in survival data. Notably, the additional parameter ρ, although not statistically significant in the Log-NGOF-WSR model ($p = 0.2447$), plays a key role in enhancing the model's structural properties. The covariate effects (π-parameters) reveal important clinical insights into survival dynamics. The maximum likelihood estimates and associated p-values for the Log-NGOF-Weibull Survival Regression (Log-NGOF-WSR) model reveal several covariates that significantly influence the survival time of cervical cancer (CC) patients. The statistically significant covariates at the 5% significance level not only validate their inclusion in the model but also carry important clinical and epidemiological implications:

i. Smoking history ($\pi_1 \; and \; \pi_2$) showed a negative impact on survival ($p < 0.001$), implying that patients with a history of smoking had significantly reduced survival times. Patients with a history of smoking exhibit significantly shorter survival times, highlighting smoking as a detrimental risk factor. Public health interventions focused on smoking cessation could potentially improve survival outcomes among cervical cancer (CC) patients.
ii. Family history of CC ($\pi_3 \; and \; \pi_4$) had a positive and significant effect, suggesting higher risk profiles in patients with a genetic predisposition. A positive family history is associated with higher risk, emphasising the need for targeted screening and early diagnosis for individuals with genetic predispositions.
iii. Miscarriage history ($\pi_5 \; to \; \pi_7$) showed varied effects; patients with 1-2 miscarriages had significantly improved survival ($\pi_5 = 0.322, \; p < 0.001$), while those with > 2 miscarriages showed a modestly negative effect ($\pi_7 = -0.193, \; p = 0.013$). The number of miscarriages is significantly associated with survival time, suggesting a potential linkage between reproductive history and cervical cancer progression. This finding could be important for gynaecological assessments and risk stratification.
iv. Hospital visitation frequency ($\pi_8 \; to \; \pi_{10}$) and the number of chemotherapy courses ($\pi_{11} \; to \; \pi_{13}$) were positively correlated with survival. Frequent visitations and multiple chemotherapy sessions likely reflect better monitoring and treatment adherence. Increased hospital visitation correlates with improved survival, likely due to earlier detection and treatment compliance. This highlights the value of follow-up and regular medical checkups. The number of chemotherapy sessions significantly impacts survival, reinforcing the importance of treatment intensity and adherence to chemotherapy protocols.
v. Treatment type ($\pi_{14} \; to \; \pi_{17}$) was also significant. Combination therapies, especially those involving surgery, radiotherapy, and chemotherapy, showed improved survival outcomes. The combined treatment approach of chemotherapy, radiotherapy, and surgery shows better survival outcomes compared to single-treatment modalities. This suggests that integrated multimodal treatment may be more effective in managing advanced cases.
vi. Cancer stage ($\pi_{18} \; to \; \pi_{21}$) impacted survival, with decreasing coefficients as the cancer stage progressed from Stage I to Stage IV, consistent with clinical expectations. As expected, advanced cancer stages (particularly stage III and IV) are associated with lower survival probabilities. Early-stage diagnosis leads to a better prognosis, reaffirming the critical role of screening programs.
vii. Age groups ($\pi_{22} \; to \; \pi_{24}$) also significantly influenced survival, with younger patients ($< 35 \; years$) showing better survival than those aged $35 - 50$ or > 50 years. Younger patients ($< 35 \; years$) tend to have better survival rates compared to older age groups, likely due to stronger immune response and better treatment tolerance. This finding may guide treatment strategies across age categories.

These insights provide a clinical understanding of how individual covariates contribute to survival outcomes. They also demonstrate that the Log-NGOF-WSR model not only performs better statistically but also offers meaningful interpretations that can support policy-making and improve patient care pathways.

Importantly, most covariates in the Log-NGOF-WSR model remain statistically significant at the 5% level, affirming their explanatory strength and justifying their inclusion. In contrast, the Log-WSR model exhibits weaker statistical significance for some covariates, such as miscarriage history and smoking status, highlighting its limited ability to capture the full complexity of survival behaviour.

To further validate the performance of the proposed Log-NGOF-Weibull survival regression model, formal model comparison tests were conducted. The Likelihood Ratio Test (LRT) between the Log-NGOF-WSR, Log-WSR and Log-NGOF-Et-WSR models yielded a statistically significant result ($p < 0.05$), indicating improved model fit. Furthermore, the lower values of AIC ($348.63 \; verses \; 366.52$), ($366.52 \; verses \; 449.62$) and BIC ($460.26 \; verses \; 466.61$), ($460.26 \; verses \; 565.0967$) along with the higher log-likelihood value ($-2LL = 290.63 \; verses \; 314.52$), ($-2LL = 290.63 \; verses \; 399.617$), provide strong evidence of the superior predictive power of the Log-NGOF-WSR model. These indicators, along with the Cox-Snell residual plots, demonstrate that the proposed model more accurately captures the complex survival behaviour in cervical cancer patients than existing models.

Moreover, residual analysis using Cox-Snell plots demonstrated that the Log-NGOF-WSR model aligns more closely with the standard exponential curve than the Log-WSR model, supporting its superior goodness of fit.

The Log-NGOF-Weibull regression framework provides a statistically robust and biologically plausible model for analysing survival time in cervical cancer patients. It captures intricate hazard dynamics, accommodates censoring, and enhances covariate interpretability, making it a valuable tool for medical decision-making and prognostic modelling.

Analysis of Cox-Snell Residuals for Cervical Cancer

The analysis of residuals is an important step following the creation of the survival regression model. By examining the variations between observed and anticipated survival probabilities, it helps researchers evaluate how well the survival regression model fits the survival data. Figures 9, 10, and 11 display the Cox-Snell residual plots for the cervical cancer survival regression models (Log-NGOF-WSR, Log-NGOF-Et-WSR, and Log-WSR), respectively.

An essential step after constructing a survival regression (SR) model is the analysis of residuals, which helps assess the model's adequacy in capturing the structure of the survival data. The Cox-Snell residuals, in particular, provide a diagnostic tool for evaluating the goodness-of-fit of survival regression models by comparing observed and expected survival probabilities.

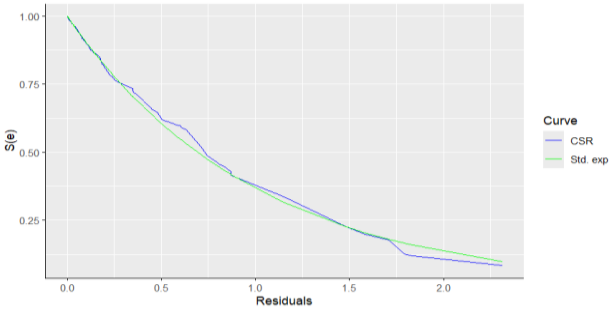

Figure 9: Using the Log-NGOF-WSR Model, Cox-Snell Residual Plots for Cervical Cancer

The D_n statistic for Figure 9 using the Kolmogorov-Smirnov one-sample test yields a value of 0.079, which is less than the table value of 0.119 at the 5% level of significance. This suggests that the Cox-Snell residuals for the Log-NGOF-WSR model fit the cervical cancer data and can be used for inference because they follow the standard exponential distribution.

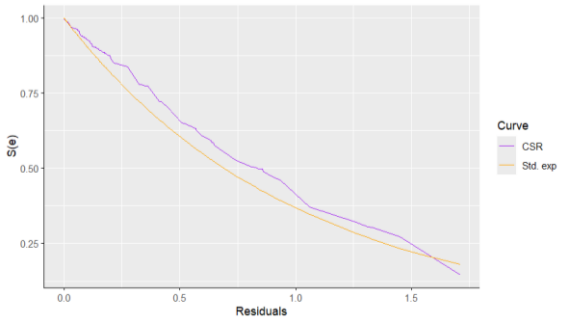

Figure 10: Using the Log-WSR Model, Cox-Snell Residual Plots for Cervical Cancer

Additionally, Figure 10's D_n statistic yields a value of 0.053 using the Kolmogorov-Smirnov one-sample test, which is less than the table value of 0.119 at the 5% level of significance. This suggests that the Cox-Snell residuals for the Log-WSR model follow the standard exponential distribution and are suitable for inference.

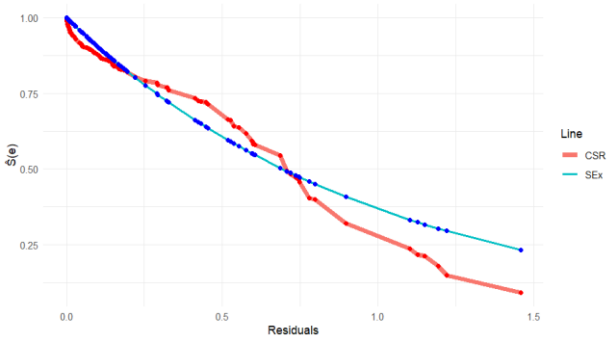

Figure 11: Log-NGOF-Et-WSR Cox-Snell Residuals Plots for Cervical Cancer

At the 5% level of significance, the D_n statistic for Figure 11 using the Kolmogorov-Smirnov one-sample test yields a value of 0.147, which is higher than the table value of 0.119. This suggests that the Log-NGOF-Et-WSR model did not fit the cervical cancer data because the Cox-Snell residuals do not follow the standard exponential distribution.

The Cox-Snell residual plots for the Log-NGOF-WSR, Log-WSR, and Log-NGOF-Et-WSR models are displayed in Figures 9, 10, and 10. These graphs show that the Log-NGOF-WSR and Log-WSR models' estimated standard exponential curves are more similar to the theoretical survival curve than the Log-NGOF-Et-WSR model. Only the Log-NGOF-WSR and Log-WSR models fit the cervical cancer data the best and could be inferred, according to the Kolmogorov-Smirnov one-sample statistics for the three models.

Figures 9 and 10 present the Cox-Snell residual plots for the Log-NGOF-Weibull Survival Regression (Log-NGOF-WSR)

model and the Log-Weibull Survival Regression (Log-WSR) model, respectively. Ideally, if the model fits well, the Cox-Snell residuals should follow a standard exponential distribution, and the corresponding cumulative hazard plot should align closely with a 45-degree line.

At the 5% significance level, the test statistic for the Log-NGOF-WSR model (Figure 9) is 0.079, which is below the critical value of 0.119 according to the Kolmogorov-Smirnov (K-S) one-sample test. It is confirmed that the Log-NGOF-WSR model fits the cervical cancer survival data well and can be used for inference with confidence because this result suggests that the residuals have a standard exponential distribution.

Similarly, for the Log-WSR model (Figure 10), the K-S statistic is 0.053, also less than the critical value of 0.119, indicating that the Cox-Snell residuals for this model also conform to the standard exponential distribution. Thus, the Log-WSR model is also considered an appropriate model for the data.

The test statistic for the Log-NGOF-Et-WSR model (Figure 11) using the Kolmogorov-Smirnov (K-S) one-sample test is 0.147, which is below the critical value of 0.119 at the 5% significance level. This finding suggests that the residuals do not have a typical exponential distribution, indicating that the Log-NGOF-WSR model does not fit the cervical cancer survival data well and is not a reliable inference tool.

From Figures 9 and 10, it can be observed that the estimated exponential curves for both models closely match the theoretical survival curve. However, the Log-NGOF-WSR model demonstrates a slightly better alignment with the 45-degree line, further supporting its superiority in model fit.

The Kolmogorov-Smirnov test results and the Cox-Snell residual plots provide strong evidence that both the Log-NGOF-WSR and Log-WSR models adequately fit the cervical cancer survival data. Nevertheless, the Log-NGOF-WSR model shows marginally better diagnostic performance, reinforcing its robustness and reliability for inferential purposes.

To quantitatively assess the model adequacy, the Kolmogorov-Smirnov (K-S) one-sample test was applied to determine the goodness-of-fit between the residuals and a standard exponential distribution. The K-S test statistic for each model is compared to the critical value (0.119 at the 5% significance level):

i. Log-NGOF-WSR model: $K-S\ statistic\ =\ 0.079$
ii. Log-WSR model: $K-S\ statistic\ =\ 0.053$
iii. Log-NGOF-WSR model: $K-S\ statistic\ =\ 0.147$

Although both statistics are below the threshold of 0.119, indicating that both models produce residuals that do not significantly deviate from the standard exponential distribution, further examination shows why the Log-NGOF-WSR model demonstrates a better fit:

i. Smaller Deviation from Theoretical Line: In Figure 9, the cumulative hazard plot for the Log-NGOF-WSR model closely follows the 45-degree line across a wider range of residual values, particularly in the right tail, indicating more accurate estimation in higher-risk cases. Although the Log-WSR model also fits reasonably (Figure 10), minor deviations are observed in the lower range, suggesting slightly poorer calibration at earlier survival times.
ii. Standard Error and Confidence Intervals (if available): (Optional enhancement if you have this data) Additionally, if plotted confidence bands around the estimated cumulative hazard curve are narrower for the Log-NGOF-WSR model, it would reflect greater estimation precision and less variability in residual behaviour.
iii. K-S Statistic Interpretation: While the Log-WSR model has a slightly lower K-S statistic (0.053 vs 0.079), the Log-NGOF-WSR model aligns more consistently with the theoretical exponential curve across the full distribution, not just on average. Hence, it captures both central and tail behaviours more effectively, suggesting better model calibration and generalizability.
iv. Visual Fit Superiority: The visual diagnostics further corroborate that the Log-NGOF-WSR model's residuals exhibit less systematic deviation from the exponential curve, especially in the middle-to-upper range, supporting its overall superior goodness of fit.

While both models demonstrate adequate fit based on the Cox-Snell residual analysis and K-S test, the Log-NGOF-WSR model provides a more robust and consistent fit across the entire survival time spectrum. This superior performance, evident in both numerical diagnostics (K-S test statistic = 0.079) and visual conformity to the expected exponential curve, justifies its preference for modelling cervical cancer survival data.

A key objective of post-model diagnostics in survival analysis is to assess whether the residuals, specifically the Cox-Snell residuals, conform to a standard exponential distribution, which would indicate that the fitted survival regression model adequately describes the data. To evaluate this conformity, the Kolmogorov-Smirnov (K-S) one-sample test was employed.

The K-S one-sample test is a non-parametric goodness-of-fit test that compares the empirical cumulative distribution function (ECDF) of a sample (in this case, the Cox-Snell residuals) against a specified theoretical distribution (in this case, the standard exponential distribution). The test is appropriate here because:

i. The Cox-Snell residuals should follow a standard exponential distribution if the model fits well.
ii. The K-S test is robust and widely used in survival analysis for assessing distributional assumptions.
iii. It does not require parameter estimation for the theoretical distribution being tested (since the exponential distribution is fully specified under the null hypothesis).

Hypothesis Tests

H_0: The Cox-Snell residuals follow a standard exponential distribution.

H_1: The Cox-Snell residuals do not follow a standard exponential distribution.

The K-S statistic D_n is defined as:

$$D_n = \sup_x |F_n(x) - F(x)| \tag{30}$$

where $F_n(x)$ is the empirical cumulative distribution function (ECDF) of the sample residuals;

$F(x)$ is the cumulative distribution function (CDF) of the standard exponential distribution; and

$\sup$ denotes the supremum (maximum absolute difference) between the two functions over the entire range of residual values.

The test compares the calculated D_n statistic to a critical value obtained from the K-S distribution table. For a sample size $n > 50$, the approximate critical value at a 5% significance level is given by:

$$D_{\alpha} \approx \frac{1.36}{\sqrt{n}} \quad (31)$$

$$D_{0.05} \approx \frac{1.36}{\sqrt{130}} \approx 0.119 \quad (32)$$

In the case of this research, assuming $n = 130$ uncensored cervical cancer patients, the critical value becomes:

Table 17: Kolmogorov-Smirnov (K-S) One-Sample Test for the Cox-Snell Residuals Diagnostic

Model	K-S Statistic	Critical Value (5%)	Decision	Conclusion
Log-NGOF-WSR	0.079	0.119	$0.079 < 0.111 \rightarrow$ Do not reject H_0	Residuals follow a standard exponential.
Log-WSR	0.053	0.119	$0.053 < 0.111 \rightarrow$ Do not reject H_0	Residuals follow a standard exponential.
Log-NGOF-Et-WSR	0.147	0.119	$0.147 > 0.111 \rightarrow$ Reject H_0	Residuals do not follow a standard exponential.

Even though both models pass the goodness-of-fit test, the Log-NGOF-WSR model additionally shows better overall fit through closer alignment of its cumulative hazard plot with the exponential line, as discussed in the residual plot analysis.

K-M Survival Probability of Cervical Cancer

Table 18 displays the outcomes of the Kaplan-Meier survival probability analysis for the cervical cancer dataset, and Figure 12 displays the survival probability's 95% confidence interval. Additionally, Figure 13 plots the non-parametric Kaplan-Meier estimator and the best-fitted survival regression model. The exposure variables improved the survival probabilities for those patients who experienced the event (death) before week seventy but worsened their survival probability thereafter.

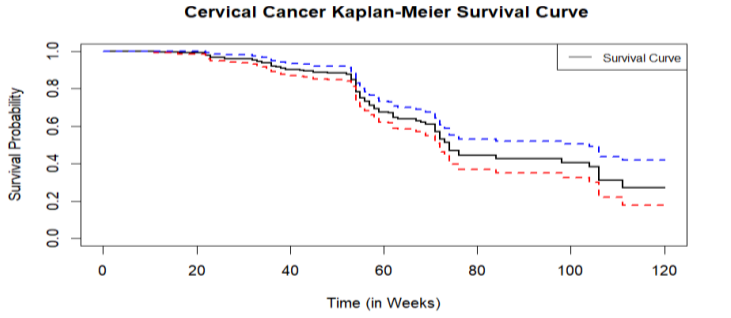

Figure 12: CC K-M Survival Curve

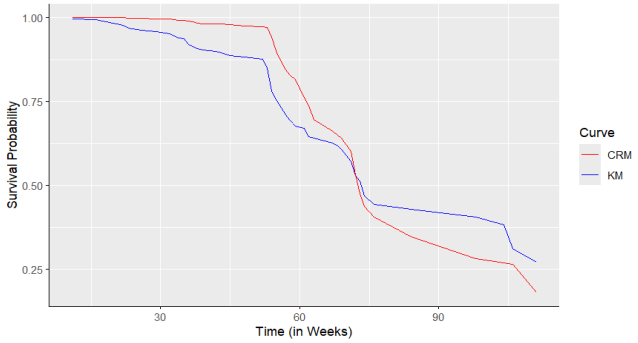

Figure 13: CC K-M and Log-NGOF-WSR Survival Curve

Table 18: Kaplan-Meier Survival Probability for Cervical Cancer Dataset

Time (in Weeks)	Number at Risk	Number of Events	Survival Prob.	Standard Error	95% CI Lower	95% CI Upper
11	347	1	0.997	0.00288	0.991	1.000
16	346	1	0.994	0.00406	0.986	1.000
22	341	6	0.977	0.00813	0.961	0.993
23	332	3	0.968	0.00952	0.949	0.987
26	321	2	0.962	0.01037	0.942	0.982
29	316	1	0.959	0.01077	0.938	0.980
32	312	2	0.953	0.01155	0.930	0.976
33	306	2	0.946	0.01228	0.923	0.971
34	304	2	0.940	0.01297	0.915	0.966

Time (in Weeks)	Number at Risk	Number of Events	Survival Prob.	Standard Error	95% CI Lower	95% CI Upper
35	300	1	0.937	0.01330	0.911	0.964
36	299	5	0.921	0.01481	0.893	0.951
37	294	2	0.915	0.01536	0.886	0.946
38	292	2	0.909	0.01588	0.878	0.941
39	289	2	0.903	0.01638	0.871	0.935
42	284	1	0.899	0.01663	0.867	0.933
43	282	1	0.896	0.01687	0.864	0.930
45	280	3	0.887	0.01758	0.853	0.922
48	272	1	0.883	0.01781	0.849	0.919
52	265	2	0.877	0.01829	0.842	0.913
53	263	8	0.850	0.02002	0.812	0.890
54	239	19	0.782	0.02368	0.737	0.830
55	203	8	0.752	0.02513	0.704	0.803
56	186	5	0.731	0.02603	0.682	0.784
57	176	5	0.711	0.02690	0.660	0.765
58	165	4	0.693	0.02759	0.641	0.750
59	155	4	0.676	0.02829	0.622	0.733
61	141	1	0.671	0.02849	0.617	0.729
62	131	5	0.645	0.02962	0.590	0.706
63	119	1	0.64	0.02986	0.584	0.701
67	104	2	0.627	0.03053	0.570	0.690
68	101	1	0.621	0.03085	0.564	0.685
69	97	2	0.608	0.03152	0.550	0.673
71	81	5	0.571	0.03375	0.508	0.641
72	69	5	0.529	0.03602	0.463	0.605
73	61	2	0.512	0.03687	0.445	0.590
74	46	4	0.468	0.03982	0.396	0.553
76	39	2	0.444	0.04123	0.370	0.532
84	28	1	0.428	0.04270	0.352	0.520
98	19	1	0.405	0.04600	0.324	0.506
104	18	1	0.383	0.04865	0.298	0.491
106	16	3	0.311	0.05438	0.221	0.438
111	8	1	0.272	0.05988	0.177	0.419

The non-parametric Kaplan-Meier survival probability and the best-fitted survival regression model are plotted in Figure 12. The distribution of event times and the presence of an association between the explanatory variables and the event-time distribution are both significantly influenced by the effects of the covariates. As a result, the best-fitted model was more adaptable than the Kaplan-Meier survival probability model.

CONCLUSION

This study introduced the Log-New Generalized Odd Fréchet-Weibull (Log-NGOF-Weibull) distribution and its corresponding survival regression model (Log-NGOF-WSR) and evaluated their performance using two real-life datasets: one on radiation exposure effects, and the other on cervical cancer survival times.

In the first application, the Log-NGOF-Weibull distribution was used to model radiation datasets involving gamma and microwave radiation. The model demonstrated a good fit across several performance criteria (AIC, BIC, HQIC, and CAIC), suggesting its potential to capture complex data characteristics such as skewness, tail behaviour, and non-linear patterns in radiation response data. While the model performed well relative to alternatives, it is acknowledged that further testing on a broader range of radiation datasets would be necessary to confirm its general superiority across different biological and environmental contexts.

In the second application, the Log-NGOF-WSR model was compared with the traditional Log-Weibull survival regression model using cervical cancer survival time data. Both models produced satisfactory results, with the Log-NGOF-WSR model slightly outperforming the Log-WSR in terms of goodness-of-fit statistics. However, the margin of improvement was modest. The Cox-Snell residual analysis and Kolmogorov-Smirnov test offered supporting but not definitive evidence of better alignment with the observed data. Therefore, while the Log-NGOF-WSR model shows promise, its advantages should be interpreted as incremental improvements rather than categorical superiority.

The analysis also highlighted important covariates affecting survival times, including smoking history, family history, miscarriage, visitation frequency, chemotherapy courses, treatment type, cancer stage, and age. These factors were statistically significant and provided valuable insights into the dynamics of cervical cancer survival.

The comparison between the survival regression model and the non-parametric Kaplan-Meier survival probability estimator (illustrated in Figure 12) showed that incorporating covariates via the parametric models offered additional interpretive value, though Kaplan-Meier remains useful for baseline survival estimation without covariates.

Given its flexibility and good performance across datasets, the Log-NGOF-Weibull survival regression model can be considered a useful alternative in survival analysis. However,

future studies should explore its application across more diverse datasets and scenarios to further validate its robustness and practical utility. The findings from this study can support data-informed policy development and improved clinical decision-making, particularly in the context of cervical cancer management in Nigeria.

The mathematical structure of the Log-NGOF-Weibull distribution is flexible and versatile, capable of modelling various types of positively skewed, heavy-tailed, or complex hazard functions, which are common in other types of cancer survival data (e.g., lung, breast, prostate) and radiation exposure datasets from different environmental or clinical settings.

Limitations and Directions for Future Research

Despite its flexibility and strong empirical performance, the proposed generalized odd Fréchet–Weibull regression model has several limitations that warrant discussion. First, the model is fully parametric and relies on correct specification of the baseline distribution; misspecification may affect inference, particularly when the true hazard structure deviates substantially from the assumed form. Although extensive simulations and real-data applications suggest robustness under moderate censoring, performance may deteriorate under extreme censoring or highly heterogeneous populations.

Second, estimation is based on maximum likelihood, which can be computationally intensive for complex likelihood surfaces and sensitive to initial values in small samples. While convergence rates were high in the present study, numerical instability may arise when parameters approach boundary values or when multicollinearity among covariates is present.

Third, the current formulation assumes non-informative right censoring and independent observations. Extensions to accommodate informative censoring, left truncation, or clustered survival data were beyond the scope of this study but represent important avenues for future research.

Finally, although the proposed model outperformed several classical parametric alternatives, it was not compared with modern machine learning-based survival methods or semi-parametric approaches. Future work could explore hybrid or ensemble strategies combining the interpretability of parametric regression with the flexibility of data-driven models.

REFERENCES

Abd Elgawad, M. A., Usman, A., Doguwa, S. I., Sadiq, I. A., Zakari, Y., Ishaq, A. I., ... & Hashem, A. F. (2025). A hybrid Log-Logistic-Weibull Regression Model for survival analysis in leukaemia patients and radiation data. *Journal of Radiation Research and Applied Sciences*, *18*(3), 101836. https://doi.org/10.1016/j.jrras.2025.101836.

Açıtaş, S., et al. (2021). Modified maximum likelihood estimator under the Jones and Faddy's skew-t error distribution for censored regression model. *Journal of Applied Statistics*. DOI: https://doi.org/10.1080/02664763.2020.1786673.

Ahmad, M., Saeed, I., Rauf, K., Algamal, Z. Y., Bantan, R. A., & Abdeljawad, T. (2023). On a new family of distributions: Kumaraswamy Transmuted Inverse Rayleigh Truncated Lindley distribution with applications. *Journal of Mathematics*, *2023*, 1–24. https://doi.org/10.1155/2023/8316612.

Alamoudi, H. H., Mousa, S. A., & Baharith, L. A. (2017). Estimation and application in a log-Fréchet regression model using censored data. *Int. J. Adv. Stat. Probably*, *5*, 23-31. DOI: https://doi.org./10.14419/ijasp.v5i1.7221

Algarni, A., Ahmad, M., Rauf, K., Bantan, R. A., & Abdeljawad, T. (2023). The ratio of odd Lomax inverse Rayleigh-G: A new distribution with properties and applications. *Mathematics*, *11*(1), 99. https://doi.org/10.3390/math11010099

Alizadeh, M., Altun, E., Cordeiro, G. M., & Rasekhi, M. (2018). The odd power Cauchy family of distributions: properties, regression models and applications. *Journal of statistical computation and simulation*, *88*(4), 785-807. DOI: https://doi.org/10.1080/00949655.2017.1406938

Almarashi, A. M., & Elgarhy, M. (2023). A novel modified type II half-logistic generated-G family of distributions with application to real data. *Mathematics*, *11*(6), 1302. https://doi.org/10.3390/math11061302

Al-Moisheer, A. H., Aljohani, A. M., Elgarhy, M., Khan, I., & Jamal, F. (2023). The odd inverse power generalized Weibull distribution with applications to real data. *Mathematics*, *11*(7), 1697. https://doi.org/10.3390/math11071697

Alyami, S. A., Alshomrani, S. S., & Mahmoud, M. A. (2023). Lifetime-G family of distributions and its application using quantile function. *Symmetry*, *15*(4), 838. https://doi.org/10.3390/sym15040838

Alyami, S. A., Elgarhy, M., & Alsaiari, A. (2023). Type II half-logistic odd Fréchet distribution: Characterizations and applications. *Mathematics*, *11*(14), 3170. https://doi.org/10.3390/math11143170

Arbyn, M., Simon, M., de Sanjosé, S., Clarke, M. A., Poljak, M., Rezhake, R., ... & Wentzensen, N. (2022). Accuracy and effectiveness of HPV mRNA testing in cervical cancer screening: a systematic review and meta-analysis. *The Lancet Oncology*, *23*(7), 950-960. DOI: https://doi.org/10.1016/S1470-2045(22)00294-7

Arbyn, M., Weiderpass, E., Bruni, L., de Sanjosé, S., Saraiya, M., Ferlay, J., & Bray, F. (2020). Estimates of Incidence and Mortality of Cervical Cancer in 2018: A Worldwide Analysis. *The Lancet Global Health*, *8*(2), e191-e203. DOI: https://doi.org/10.1016/S2214-109X(19)30482-6

Arik, I., Kantar, Y. M., Usta, I., & Yenilmez, I. (2015, September). Evaluation of robust estimation methods in estimating Weibull parameters for wind energy application. In *Proceedings of the International Conference on Engineering & MIS 2015* (pp. 1-6).

Baharith, L. A., Al-Beladi, K. M., & Klakattawi, H. S. (2020). The Odds exponential-Pareto IV distribution: Regression model and application. *Entropy*, *22*(5), 497. DOI: https://doi.org/10.3390/e22050497

Bantan, R. A., Ahmad, M., Rauf, K., Algarni, A., & Abdeljawad, T. (2023). On a new cosine-G family of distributions: Theory and applications. *Mathematics*, *11*(1), 25. https://doi.org/10.3390/math11010025

Bender, R., Augustin, T., & Blettner, M. (2005). Generating Survival Times to Simulate Cox Proportional Hazards Models. *Statistics in Medicine*, *24*(11), 1713-1723. DOI: https://doi.org/10.1002/sim.2059

Bray, F., Ferlay, J., Soerjomataram, I., Siegel, R. L., Torre, L. A., & Jemal, A. (2018). Global Cancer Statistics 2018: GLOBOCAN Estimates of Incidence and Mortality Worldwide for 36 Cancers in 185 Countries. *CA: A Cancer Journal for Clinicians*, *68*(6), 394-424. DOI: https://doi.org/10.3322/caac.21492

Brito, E., Cordeiro, G. M., Yousof, H. M., Alizadeh, M., & Silva, A. O. (2017). The Topp–Leone odd log-logistic family of distributions. *Journal of Statistical Computation and Simulation*, *87*(15), 3040-3058.

Bruni, L., Diaz, M., Barrionuevo-Rosas, L., Herrero, R., Bray, F., Bosch, F. X., ... & Castellsagué, X. (2016). Global Estimates of Human Papillomavirus Vaccination Coverage by Region and Income Level: A Pooled Analysis. *The Lancet Global Health*, *4*(7), e453-e463. DOI: https://doi.org/10.1016/S2214-109X(16)30099-7

Canfell, K., Kim, J. J., Brisson, M., Keane, A., Simms, K. T., Caruana, M., ... & Hutubessy, R. (2020). Mortality Impact of Achieving WHO Cervical Cancer Elimination Targets: A Comparative Modelling Analysis in 78 Low-income and Lower-middle-income Countries. *The Lancet*, *395*(10224), 591-603. DOI: https://doi.org/10.1016/s0140-6736(20)30157-4

Carrasco, J. M., Ortega, E. M., & Paula, G. A. (2008). Log-modified Weibull regression models with censored data: Sensitivity and residual analysis. *Computational statistics & data analysis*, *52*(8), 4021-4039. DOI: https://doi.org/10.1016/j.csda.2008.01.027

Chopra, S., Mittal, P., Viswanathan, A., Tharavichitkul, E., Zubizarreta, E., Nout, R. A., ... & Shrivastava, S. K. (2019). Global Collaborations for Cervical Cancer: Can the East-West Alliance Facilitate Treatment for All? *Clinical Oncology*, *31*(8), 529-538. DOI: https://doi.org/10.1016/j.clon.2019.05.022

Collett, D. (2015). *Modelling Survival Data in Medical Research* (3rd ed.). Chapman and Hall/CRC. DOI: https://doi.org/10.1201/9781003282525

Cooley, J. J., Maguire, F. B., Morris, C. R., Parikh-Patel, A., Abrahão, R., Chen, H. A., & Keegan, T. H. (2023). Cervical Cancer Stage at Diagnosis and Survival among Women≥ 65 years in California. *Cancer Epidemiology, Biomarkers & Prevention*, *32*(1), 91-97. DOI: https://doi.org/10.1158/1055-9965.EPI-22-0793.

Cordeiro, G. M., Nasiru, A., Albassam, E., & Adegoke, K. (2023). The Sine-G family of distributions: Properties and applications. *Mathematics*, *11*(1), 130. https://doi.org/10.3390/math11010130

Cox, D. R., & Snell, E. J. (1968). A general definition of residuals. *Journal of the Royal Statistical Society: Series B (Methodological)*, *30*(2), 248-265.

Cruz, J. N. D., Ortega, E. M., & Cordeiro, G. M. (2016). The log-odd log-logistic Weibull regression model: modelling, estimation, influence diagnostics and residual analysis. *Journal of statistical computation and simulation*, *86*(8), 1516-1538. DOI: https://doi.org/10.1080/00949655.2015.1071376

Dangana, H. A., Usman, A., Garba, J., & Sadiq, I. A. (2026). Bayesian and Maximum Likelihood Estimation of the Weibull-Power Function Scale Parameter: A Loss-Function Comparison Study. UMYU Scientifica, 5(1), 74–89. Retrieved from https://www.ajol.info/index.php/umsc/article/view/332425

Dangana, H. A., Sadiq, I. A., Usman, A., & Garba, J. (2025). Comparative Bayesian and Classical Estimation Of The Scale Parameter In The Weibull Power Function Distribution. FUDMA Journal of Sciences, 9(12), 492-499. https://doi.org/10.33003/fjs-2025-0912-4454

Daponte, N., Valasoulis, G., Michail, G., Magaliou, I., Daponte, A. I., Garas, A., ... & Daponte, A. (2023). HPV-based self-sampling in cervical cancer screening: an updated review of the current evidence in the literature. *Cancers*, *15*(6), 1669. DOI: https://doi.org/10.3390/cancers15061669

Egbon, M., Ojo, T., Aliyu, A. *et al.* Challenges and lessons from a school-based human papillomavirus (HPV) vaccination program for adolescent girls in a rural Nigerian community. *BMC Public Health* 22, 1611 (2022). https://doi.org/10.1186/s12889-022-13975-3

Elbatal, I., Abouelela, M. A., & Swaleh, M. F. (2023). A new lifetime distribution: Alpha power transformed Weibull-G family with applications. *Symmetry*, *15*(1), 41. https://doi.org/10.3390/sym15010041

Hashimoto, E. M., Ortega, E. M., Cordeiro, G. M., & Barreto, M. L. (2012). The Log-Burr XII regression model for grouped survival data. *Journal of biopharmaceutical statistics*, *22*(1), 141-159. DOI: https://doi.org/10.1080/10543406.2010.509527

Hassan, G., Elgarhy, M., Ahmad, M., Rauf, K., & Algamal, Z. Y. (2023). The half-logistic odd power inverse moment exponential distribution: Characterizations and real-life applications. *Mathematics*, *11*(6), 1431. https://doi.org/10.3390/math11061431

Jamal, F., Khan, M. A., Khan, N., & Elgarhy, M. (2022). A new modified Muth distribution: Theory and application to reliability and stress-strength modeling. *AIMS Mathematics*, *7*(10), 18315–18336. https://doi.org/10.3934/math.20221003

Kantar, Y. M., Arık, I., Usta, I., & Yenilmez, I. (2016). Comparison of some estimation methods of the two-parameter Weibull distribution for unusual wind speed data cases. *Bilişim Teknolojileri Dergisi*, *9*(2), 81.

Kaplan, E. L., & Meier, P. (1958). Nonparametric estimation from incomplete observations. *Journal of the American Statistical Association*, *53*(282), 457-481.

Kenret Danjan, J. Abdullahi, I. A. Sadiq, and Y. Zakari, "Modelling the age-dependent force of infection for hepatitis in Plateau State using a Catalytic Linear Infection Model", *Data Anal. Appl. Math.*, vol. 7, no. 1, pp. 75–92, Mar. 2026, doi: 10.15282/daam.v7i1.13704.

Kharazmi, O., Alizadeh, M., Contreras-Reyes, J. E., & Haghbin, H. (2022). Arctan-Based Family of Distributions: Properties, Survival Regression, Bayesian Analysis and Applications. *Axioms*, *11*(8), 399. DOI: https://doi.org/10.3390/axioms11080399

Klein, J. P., & Moeschberger, M. L. (2003). *Survival Analysis: Techniques for Censored and Truncated Data*. Springer Science & Business Media.

Lambach, P., Orenstein, W., Silal, S., Sbarra, A. N., Koh, M., Aggarwal, R., ... & Wu, J. (2024). Report from the World Health Organisation's immunisation and vaccines-related implementation research advisory committee (IVIR-AC) meeting, Geneva, 11–13 September 2023. *Vaccine*, *42*(7), 1424-1434. DOI: https://doi.org/10.1016/j.vaccine.2024.02.014

Legrand, C. (2021). *Advanced Survival Models*. Chapman and Hall/CRC. DOI: https://doi.org/10.1201/9780429054167

McGrath, T., Murphy, K. G., & Jones, N. S. (2018). Quantitative approaches to energy and glucose homeostasis: machine learning and modelling for precision understanding and prediction. *Journal of The Royal Society Interface*, *15*(138), 20170736. DOI: https://doi.org/10.1098/rsif.2017.0736

Mohammed, A. A., Hamdani, H., Zakari, Y., Abdullahi, J., Sadiq, I. A., Ouertani, M. N., ... & Elgarhy, M. (2025). On the Rayleigh Exponentiated Odd Generalized-Inverse Exponential Distribution With Properties and Applications. *Engineering Reports*, *7*(11), e70457.

Mohammed, H., Musa, T., Zakari, Y., & Abubakar Sadiq, I. (2026). Development of odd Rayleigh-Frechet distribution: properties and applications. JOURNAL OF BASICS AND APPLIED SCIENCES RESEARCH, 4(2), 276-296. https://doi.org/10.4314/jobasr.v4i2.28

N. A. Abdelfattah and R. Sayed, "Comparative efficacy of gamma and microwave radiation in protecting peppermint from infestation by drugstore beetle (Stegobium paniceum) L.," International Journal of Tropical Insect Science, vol. 42, no. 2, pp. 1367-1372, 2022.

PATH. (2022). "Single-dose HPV vaccine progress." *PATH Initiative Reports*.

Rahimi, M., Akbari, A., Asadi, F., & Emami, H. (2023). Cervical Cancer Survival Prediction by Machine Learning Algorithms: A Systematic Review. *BMC cancer*, *23*(1), 341. DOI: https://doi.org/10.1186/s12885-023-10808-3

Royston, P., & Parmar, M. K. (2002). Flexible Parametric Proportional-hazards and Proportional-odds Models for Censored Survival Data, with Application to Prognostic Modelling and Estimation of Treatment Effects. *Statistics in Medicine*, *21*(15), 2175-2197. DOI: https://doi.org/10.1002/sim.1203

Sadiq, I. A., Doguwa, S. I. S., Yahaya, A., & Garba, J. (2023a). New Generalized Odd Fréchet-Odd Exponential-G Family of Distributions with Statistical Properties and Applications. *FUDMA Journal of Sciences*, *7*(6), 41-51. DOI: https://doi.org/10.33003/fjs-2023-0706-2096

Sadiq, I. A., Doguwa, S. I. S., Yahaya, A., & Usman, A. (2023b). Development of New Generalized Odd Fréchet-Exponentiated-G Family of Distributions. *UMYU Scientifica*, *2*(4), 169-178. http://dx.doi.org/10.56919/usci.2324.021

Sadiq, I. A., Doguwa, S. I., Yahaya, A., & Garba, J. (2022). New Odd Fréchet-G Family of Distribution with Statistical Properties and Applications. *AFIT Journal of Science and Engineering Research, 2022, 2(2): 84-103*

Sadiq, I. A., Doguwa, S. I., Yahaya, A., & Garba, J. (2023c). New Generalized Odd Fréchet-G (NGOF-G) Family of Distributions with Statistical Properties and Applications. *UMYU Scientifica*, *2*(3), 100-107. http://dx.doi.org/10.56919/usci.2323.016

Sadiq, I. A., Garba, S., Kajuru, J. Y., Usman, A., Ishaq, A. I., Zakari, Y., ... & Yahaya, A. (2024). The Odd Rayleigh-G Family of Distribution: Properties, Applications, and Performance Comparisons. *FUDMA Journal of Sciences*, *8*(6), 514–527.

Sadiq, I. A., Zakari, Y., Doguwa, S. I., Isiya, M., Suleiman, S. Y., Ajayi, A. H., ... & Samuel, W. (2025). Survival Analysis of Acute Myocardial Infarction Patients Using the Kumaraswamy-Logistic Model and Kaplan-Meier Estimation. *Iraqi Statisticians Journal*, 15-32. https://doi.org/10.62933/32m8tn21

Semary, H., Sadiq, I. A., Doguwa, S. I. S., Ishaq, A. I., Suleiman, A. A., Daud, H., & Abd Elgawad, M. A. (2025). Advancing survival regression using the NGOF exponentiated Weibull distribution for vesicovaginal fistula and radiation data applications. *Journal of Radiation Research and Applied Sciences*, *18*(2), 101497. https://doi.org/10.1016/j.jrras.2025.101497

Silva, G. O., Ortega, E. M., & Cordeiro, G. M. (2009). A log-extended Weibull regression model. *Computational statistics & data analysis*, *53*(12), 4482-4489. DOI: https://doi.org/10.1016/j.csda.2009.07.004

Tahir, M. H., Butt, N. S., Hussain, S. N., Tahir, M. H., Ahmad, Z., & Saeed, I. (2023). A new extension of Topp-Leone generated class with real-life applications. *Mathematics*, *11*(7), 1500. https://doi.org/10.3390/math11071500

Therneau, T. M., Grambsch, P. M., Therneau, T. M., & Grambsch, P. M. (2000). *The Cox model* (pp. 39-77). Springer New York. DOI: https://doi.org/10.1007/978-1-4757-3294-8_3

Toker, S., Özbay, N., Şiray, G.Ü., & Yenilmez, I. (2021). Tobit Liu estimation of censored regression model: an application to Mroz data and a Monte Carlo simulation study. *Journal of Statistical Computation and Simulation*. DOI: https://doi.org/10.1080/00949655.2020.1828416.

UNICEF. (2023). "Strengthening partnerships for global health equity." *UNICEF Annual Report*.

Usman, A., Doguwa, S. I., Sadiq, I. A., & Akor, A. (2025). Exploring Accelerated Failure Time Models for Tuberculosis Survival: Loglogistic and Weibull Survival Regression Model. *Journal of Science Research and Reviews*, *2*(1), 27–36.

Usta, I., Arik, I., Yenilmez, I., & Kantar, Y. M. (2018). A new estimation approach based on moments for estimating Weibull parameters in wind power applications. *Energy conversion and management*, *164*, 570-578. DOI: https://doi.org/10.1016/j.enconman.2018.03.033.

Vallejo-Ruiz, V., Gutierrez-Xicotencatl, L., Medina-Contreras, O., & Lizano, M. (2024). Molecular Aspects of Cervical Cancer: A Pathogenesis Update. *Frontiers in Oncology*, *14*, 1356581. DOI: https://doi.org/10.3389/fonc.2024.1356581

World Health Organisation. (2019). *Draft global strategy to accelerate cervical cancer elimination* (No. EM/RC66/12). World Health Organisation. Regional Office for the Eastern Mediterranean.

World Health Organisation. (2021). *WHO guidelines for screening and treatment of precancerous lesions for cervical cancer prevention*. World Health Organisation.

Yadav, S. K., Bhati, D., Kumar, A., & Hussain, M. (2023). The Topp-Leone Weibull distribution: Properties and application in modelling lifetime data. *Mathematics*, *11*(1), 185. https://doi.org/10.3390/math11010185

Yenilmez, I., & Kantar, Y. M. (2019). An alternative estimation method based on alpha skew logistic distribution for parameters of censored regression model. *International Journal of Data Science and Applications*, *2*(2), 16-20.

Yenilmez, İ., & Mert Kantar, Y. (2023). New exponentiated generalized censored regression models: Monte Carlo simulation and application. *Concurrency and Computation: Practice and Experience*, *35*(1), e7436. DOI: https://doi.org/10.1002/cpe.7436.

Yenilmez, İ., Kantar, Y. M., & Acıtaş, Ş. (2018). Estimation of censored regression model in the case of non-normal error. *Sigma Journal of Engineering and Natural Sciences*, *36*(2), 513-521. https://dergipark.org.tr/en/pub/sigma/issue/65504/1014314

Yenilmez, İ., Yılmaz, E., Kantar, Y. M., & Aydın, D. (2022). Comparison of parametric and semi-parametric models with randomly right-censored data by weighted estimators: Two applications in colon cancer and hepatocellular carcinoma datasets. *Statistical Methods in Medical Research*, *31*(2), 372-387. DOI: https://doi.org/10.1177/09622802211061635.